INL/CON-23-71110-Revision-1

The Performance of FBMC-SS in Challenging HF Channel Environments

February 2023

Brandon Hunt, David Haab, Behrouz Farhang-Boroujeny, Thomas Cameron Sego, Tom Holschuh, Hussein Moradi

Changing the World's Energy Future

INL is a U.S. Department of Energy National Laboratory operated by Battelle Energy Alliance, LLC

DISCLAIMER

This information was prepared as an account of work sponsored by an agency of the U.S. Government. Neither the U.S. Government nor any agency thereof, nor any of their employees, makes any warranty, expressed or implied, or assumes any legal liability or responsibility for the accuracy, completeness, or usefulness, of any information, apparatus, product, or process disclosed, or represents that its use would not infringe privately owned rights. References herein to any specific commercial product, process, or service by trade name, trade mark, manufacturer, or otherwise, does not necessarily constitute or imply its endorsement, recommendation, or favoring by the U.S. Government or any agency thereof. The views and opinions of authors expressed herein do not necessarily state or reflect those of the U.S. Government or any agency thereof.

INL/CON-23-71110-Revision-1

The Performance of FBMC-SS in Challenging HF Channel Environments

Brandon Hunt, David Haab, Behrouz Farhang-Boroujeny, Thomas Cameron Sego, Tom Holschuh, Hussein Moradi

February 2023

Idaho National Laboratory
Idaho Falls, Idaho 83415

http://www.inl.gov

Prepared for the
U.S. Department of Energy
Under DOE Idaho Operations Office
Contract DE-AC07-05ID14517

The Performance of FBMC-SS in Challenging HF Channel Conditions

Idaho National Laboratory and The University of Utah

Brandon Hunt, Thomas Cameron Sego,
David B. Haab, Thomas V. Holschuh,
Hussein Moradi, and Behrouz Farhang-Boroujeny

Battelle Energy Alliance manages INL for the
U.S. Department of Energy's Office of Nuclear Energy

Idaho National Laboratory

Outline

- Provide overview of FBMC-SS waveform
  - Transmitter structure
  - NMF-based receiver structure
  - Discuss spectrum and bandwidth
- Present simulated results in challenging channel environments
  - Cases:
    - 2 path channel with 2nd path frequency offset
    - 2 path mid-latitude disturbed and “very poor” channels
    - Large narrowband interferer
    - Highly congested interference case
    - Highly dynamic interference case
- Conclusion

FBMC-SS transmitter

- Filter bank multicarrier spread-spectrum (FBMC-SS)
  - Symbols spread over K non-overlapping adjacent subcarriers
  - Waveform can be optimized to have low PAPR ($\mathrm{PAPR} < 4.5\ \mathrm{dB}$)

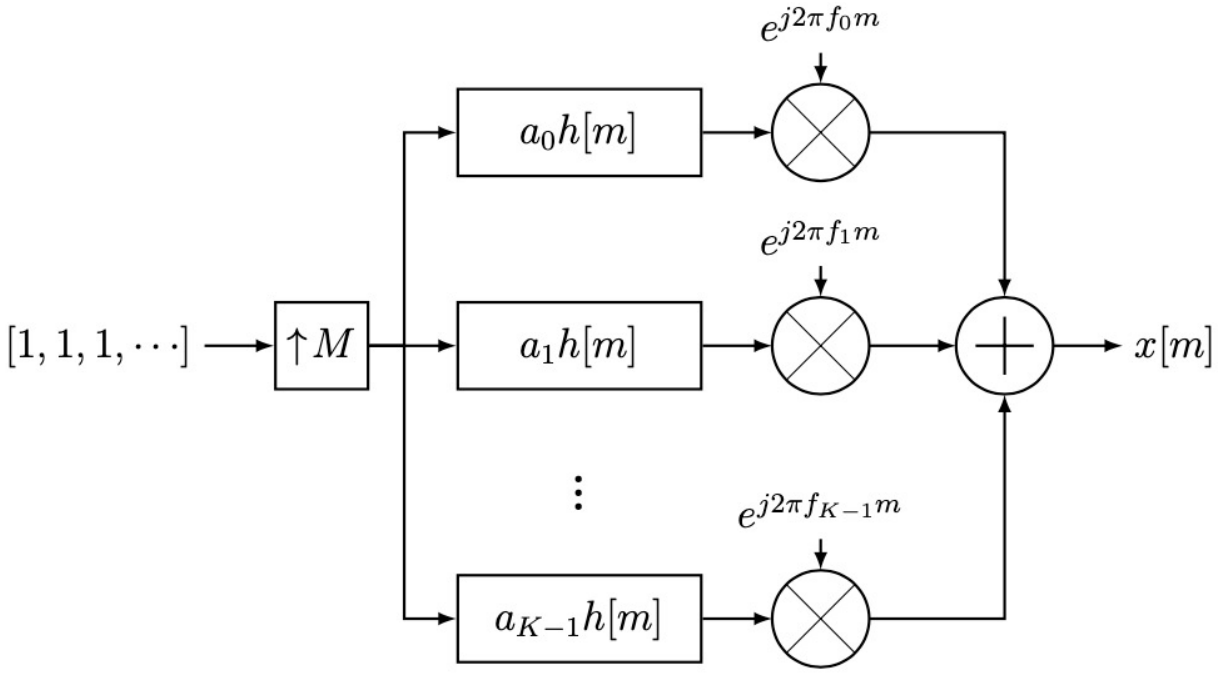

Figure 1: FBMC-SS transmitter structure

FBMC-SS transmitter

- Data is encoded along subcarrier phases using multicodes
  - $a_k = \gamma_{k,n}\theta_{k,n}$
  - $\gamma_{k,n}$: spreading gain for k-th subcarrier at symbol time n
  - $\theta_{k,n}$: the spread-spectrum 'chip' for k-th subcarrier at symbol time n

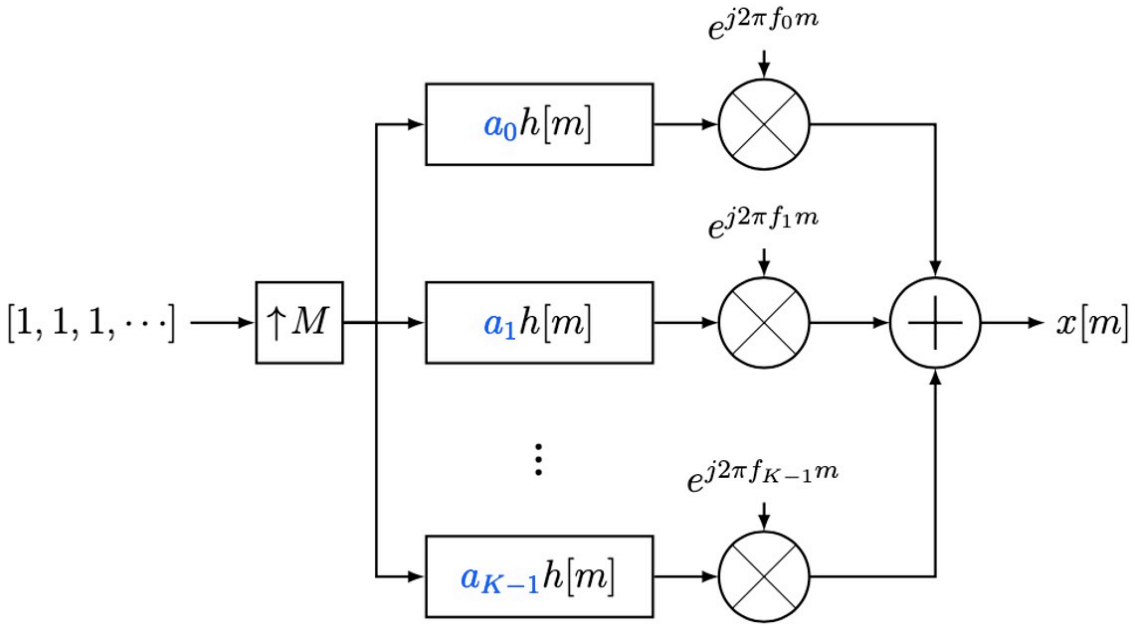

Figure 1: FBMC-SS transmitter structure; multicode 'chips' are written in blue.

FBMC-SS receiver

- Normalized Matched-Filter (NMF) [1]
  - Matched filtering with blind subcarrier normalization
  - Blindly approximates maximum ratio combining
- Improved packet detection in presence of high partial-band interference
- Efficient implementation with overlap-add method

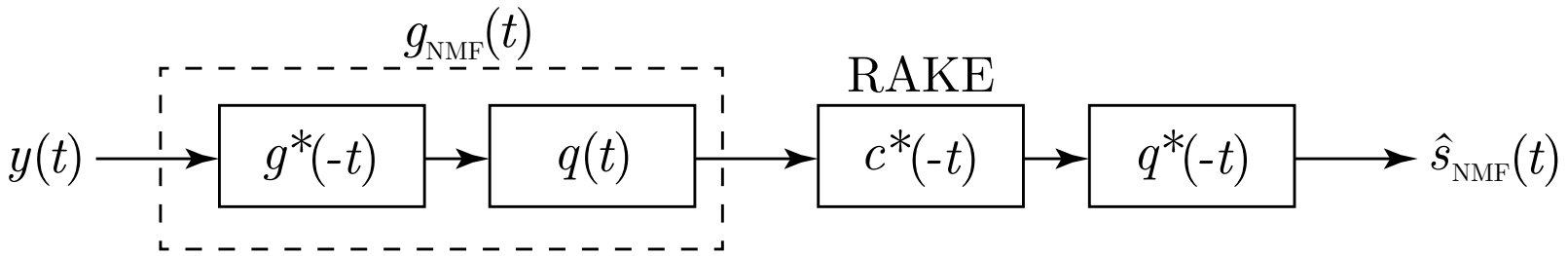

Figure 2: Basic NMF Receiver structure

[1] D. B. Haab, H. Moradi, and B. Farhang-Boroujeny, "Spread Spectrum Symbol Detection With Blind Interference Suppression in FBMC-SS," in IEEE Open Journal of the Communications Society, vol. 2, pp. 1630 1646, 2021, doi: 10.1109/OJCOMS.2021.3090356.

FBMC-SS receiver

- Additional receiver details:
  - Preamble detector tests multiple candidate Carrier Frequency Offsets (CFO)
    - This improves packet detection in presence of large CFO
  - Inserted pilots allow for detection of additional modes of propagation
  - Different spreading gains applied to each symbol reduce the impact of inter-symbol interference (ISI)

FBMC-SS waveform parameters

- Parameters chosen based on [2] to match MIL-STD-188-110D, WFID 0 (Walsh), 48 kHz waveform
  - Direct sequence spread-spectrum
- Receiver given no channel information; same receiver settings used for each case

Table 1: Waveform parameters

Parameter	Value
Number subcarriers	40
Symbol rate	600 sym/sec
Subcarrier bandwidth	1200 Hz
Null-to-null bandwidth	48 kHz
Modulation order	4 bits/sym
Modulation type	Orthogonal
Inserted pilot rate	1 pilot every 6 data syms
Payload size	2048 bits

[2] J. Nieto, W. Furman, W. Batts, “A Comparison of Published Waveform Design Techniques Used for Reliable HF Communications,” Proceedings of the Nordic HF Conference HF22, 2022.

FBMC-SS waveform parameters

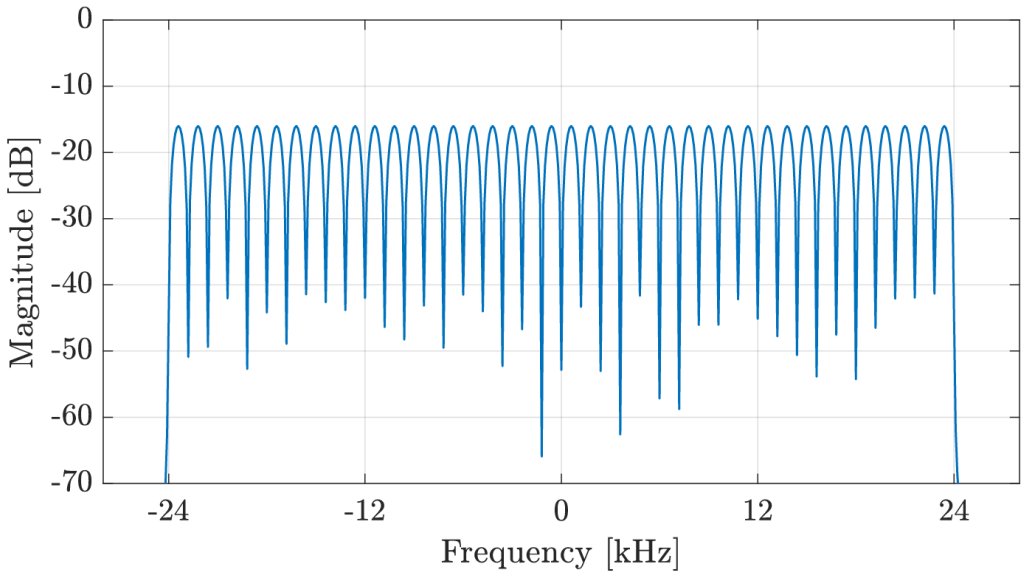

Figure 3: Frequency response of transmit pulse-shaping filter with parameters given in Table 1

Table 1: Waveform parameters

Parameter	Value
Number subcarriers	40
Symbol rate	600 sym/sec
Subcarrier bandwidth	1200 Hz
Null-to-null bandwidth	48 kHz
Modulation order	4 bits/sym
Modulation type	Orthogonal
Inserted pilot rate	1 pilot every 6 data syms
Payload size	2048 bits

Bandwidths

- MIL-STD-188-110D defines bandwidth as the width in frequency containing 99% of the signal power.
- Following this definition, for a nominal bandwidth of 48 kHz, the 99% bandwidth is:
  - $W_{\mathrm{Walsh}} = 44{,}700$ Hz
- For the associated FBMC-SS waveform,
  - $W_{\mathrm{FBMC-SS}} = 47{,}150$ Hz

Bandwidths (cont.)

- 99.74% of the signal energy is contained in the same bandwidth for both waveforms

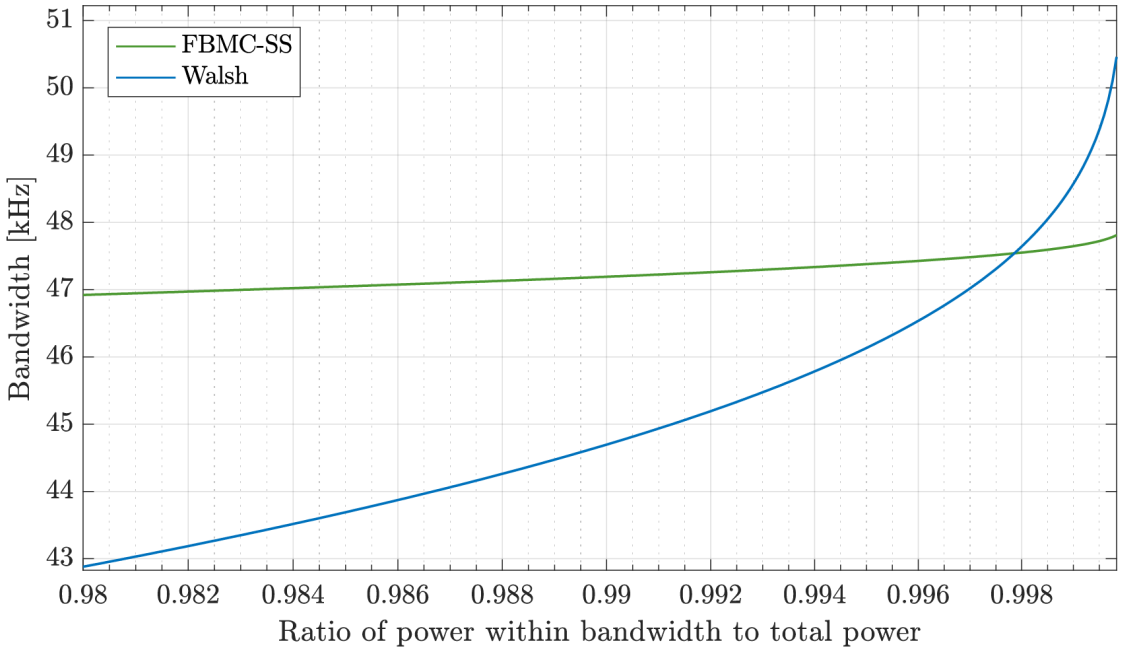

Figure 4: Signal bandwidth as function of ratio of power within bandwidth

Bandwidths (cont.)

- 99.74% of the signal energy is contained in the same bandwidth for both waveforms
  - At this point, the bandwidth is $W_{99.74\%} = 47.5$ kHz
  - This point remains below the nominal bandwidth of 48 kHz

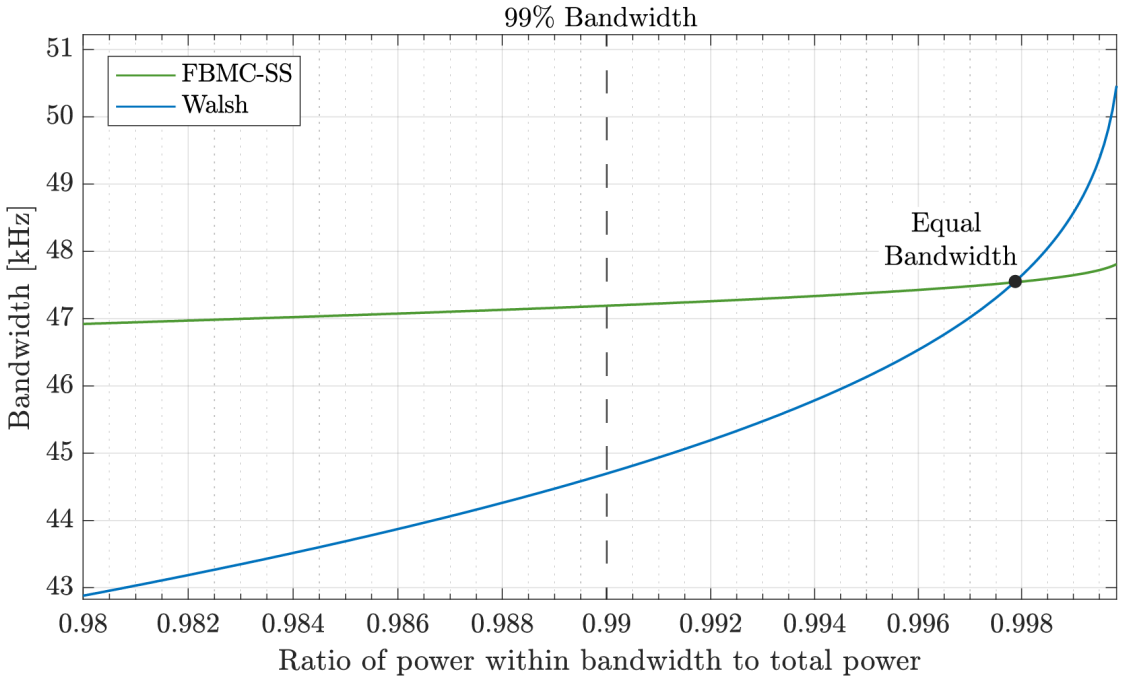

Figure 4: Signal bandwidth as function of ratio of power within bandwidth

Bandwidths (cont.)

- 99.74% of the signal energy is contained in the same bandwidth for both waveforms
  - At this point, the bandwidth is $W_{99.74\%} = 47.5$ kHz
  - This point remains below the nominal bandwidth of 48 kHz
  - For FBMC-SS, nearly all signal power is confined to 48 kHz
    - Improved adjacent channel rejection

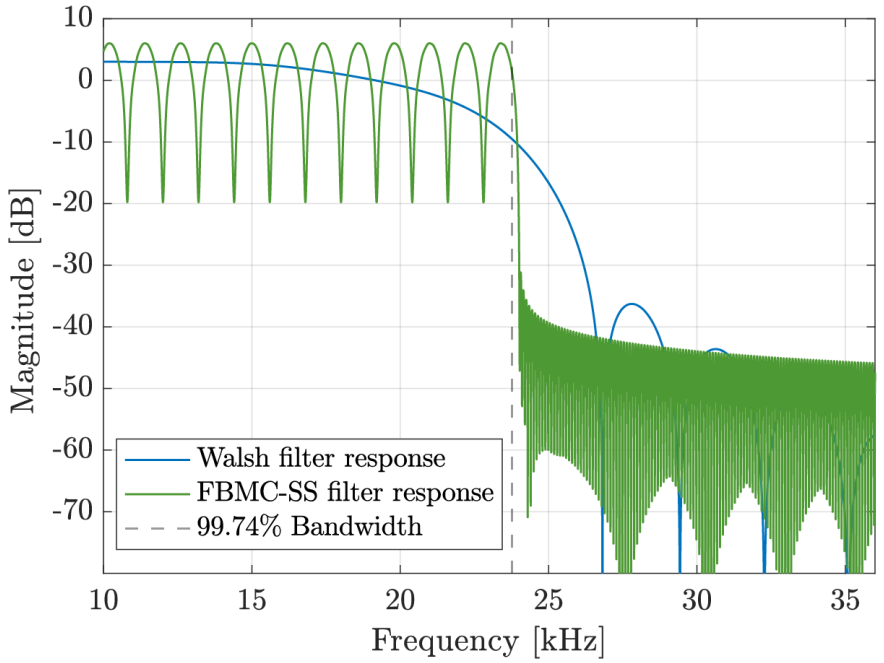

Figure 5: Power spectral density of Walsh and FBMC-SS transmit pulse-shaping filters

Simulated channels

- Several HF channel conditions are simulated, following [2]:
  - 2 path frequency offset channel
    - $N_{\text{path}} = 2, T_d = 2$ ms, $f_{\text{path \#2}} = \{0, 1, 10, 25\}$ Hz

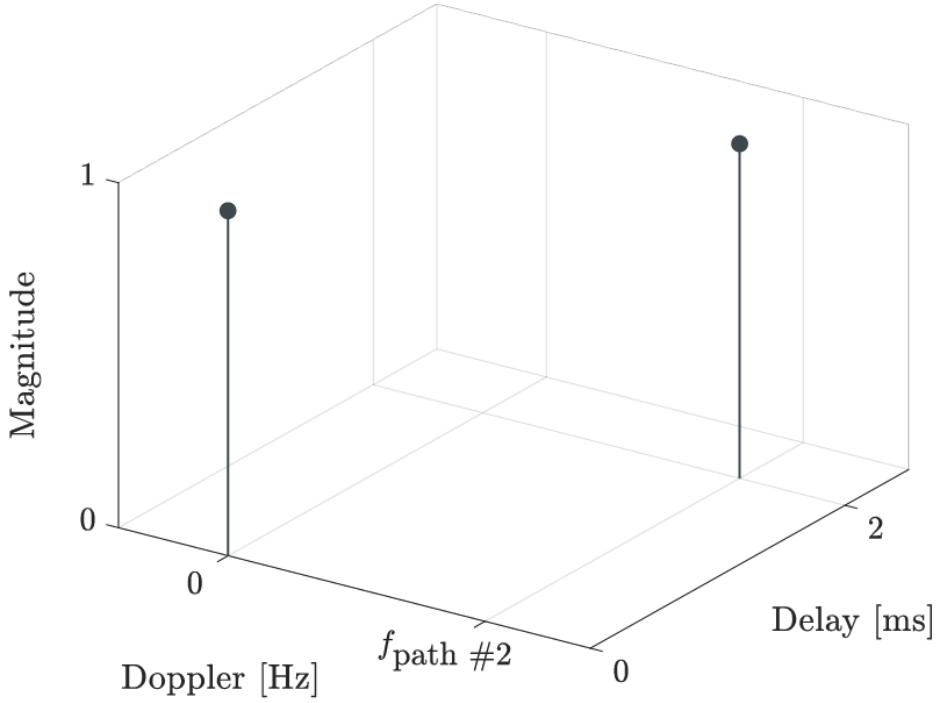

Figure 6: Delay-Doppler representation of 2 path, frequency offset channel

Simulated channels

- Several HF channel conditions are simulated, following [2]:
  - 2 path frequency offset channel
    - $N_{\text{path}} = 2, T_d = 2$ ms, $f_{\text{path \#2}} = \{0, 1, 10, 25\}$ Hz
  - 2 path Mid Latitude Disturbed (MLD) and "Very Poor" (VP) channels [3]
    - $N_{\text{path}} = 2, T_d = 2$ ms, $D_s = \{1, 10\}$ Hz

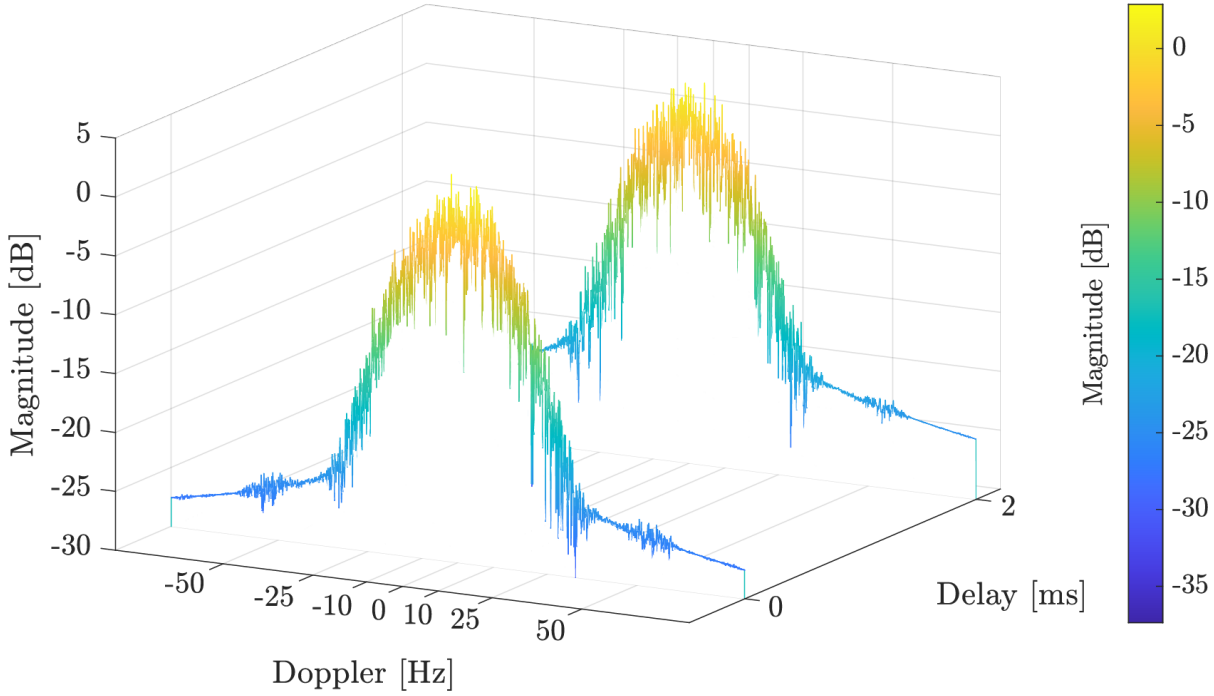

Figure 7: Delay-Doppler representation of VP channel

[3] ITU-R Recommendation F.1487, "Testing of HF modems with bandwidths of up to about 12 kHz using Ionospheric channel simulators," 2000

Simulated channels

- Several HF channel conditions are simulated, following [2]:
  - 2 path frequency offset channel
    - $N_{\text{path}} = 2, T_d = 2$ ms, $f_{\text{path \#2}} = \{0, 1, 10, 25\}$ Hz
  - 2 path Mid Latitude Disturbed (MLD) and "Very Poor" (VP) channels [3]
    - $N_{\text{path}} = 2, T_d = 2$ ms, $D_s = \{1, 10\}$ Hz
  - Ideal channel with narrowband interference
    - $N_{\text{path}} = 1, P_{\text{intf}} = \{-\infty, 15, 50\}$ dB

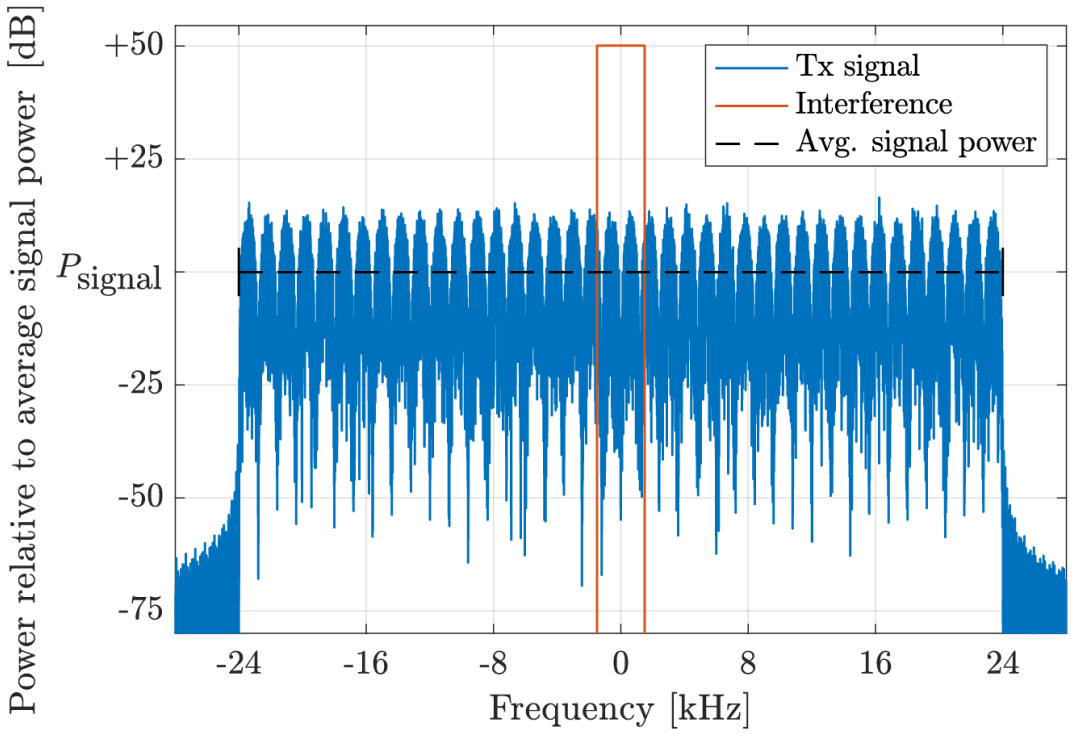

Figure 8: Power spectral densities of signal and interference for $P_{\text{intf}} = 50$ dB

Results legend

- Results for each transceiver system are color coded

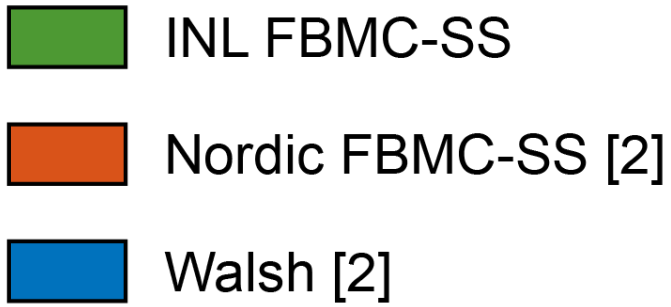

Table 2: Example color-coded table containing results

Waveform Type	Result
INL FBMC-SS	Result 1
Nordic FBMC-SS	Result 2
Walsh	Result 3

Results legend

- Results for each transceiver system are color coded

INL FBMC-SS

Nordic FBMC-SS [2]

Walsh [2]

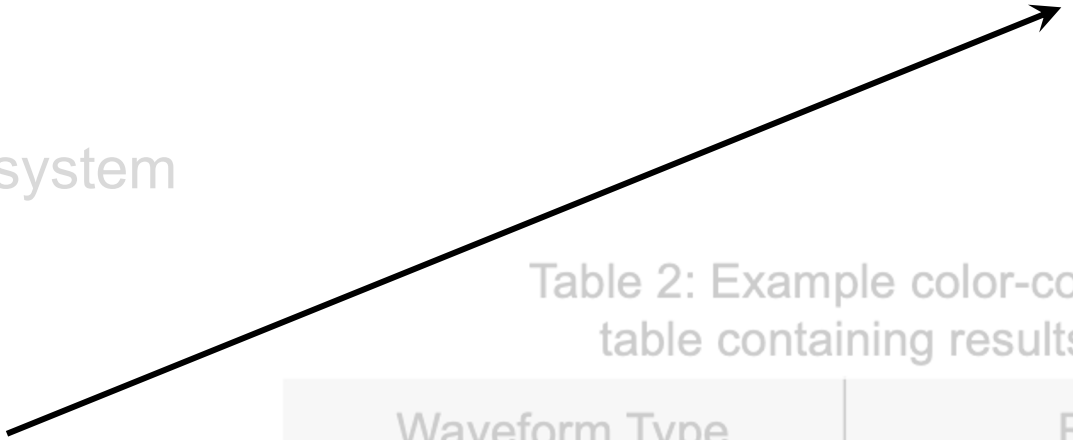

INL FBMC-SS

Nordic FBMC-SS [2]

Walsh [2]

Table 2: Example color-coded table containing results

Waveform Type	Result
INL FBMC-SS	Result 1
Nordic FBMC-SS	Result 2
Walsh	Result 3

Results for 2 path, freq. offset channel

INL FBMC-SS
Nordic FBMC-SS [2]
Walsh [2]

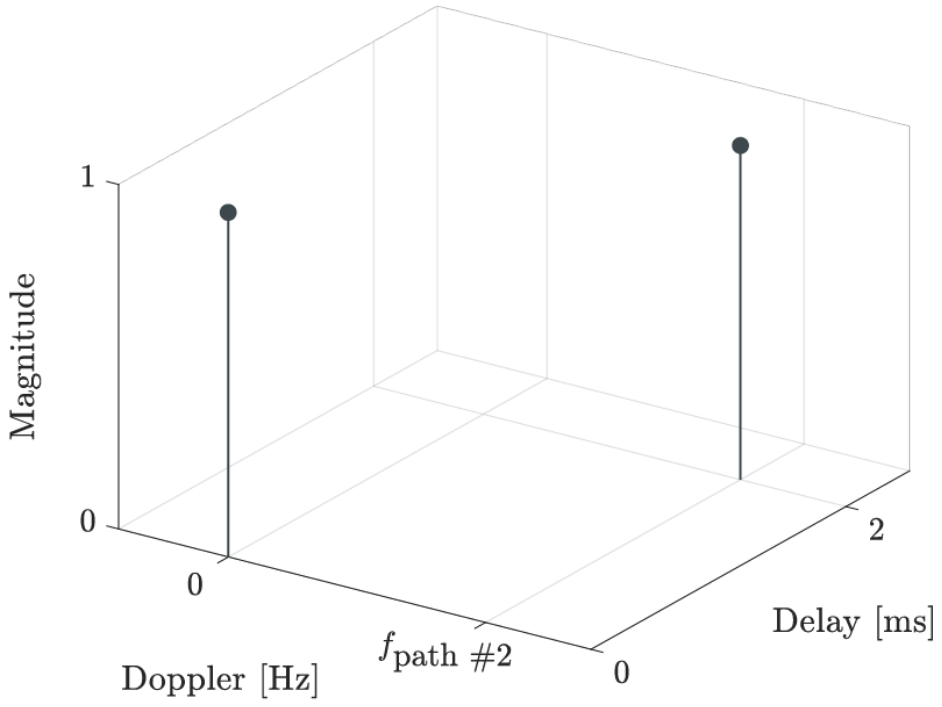

Figure 6: Delay-Doppler representation of simulated channel

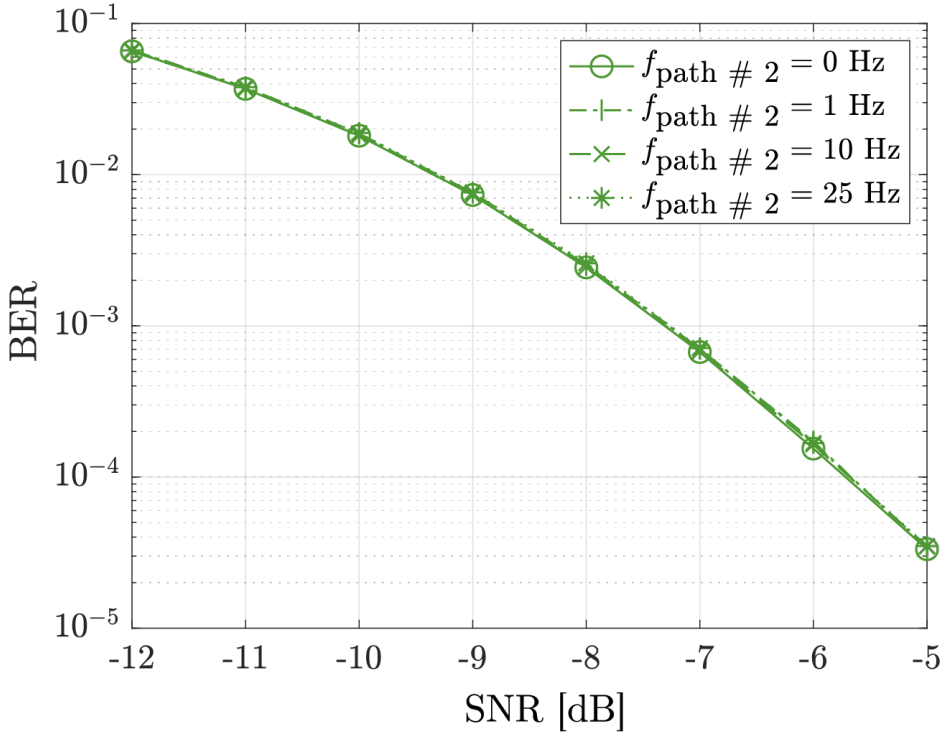

Figure 9: INL FBMC-SS waveform performance in 2 path channel with 2nd path frequency offset

Results for 2 path, freq. offset channel

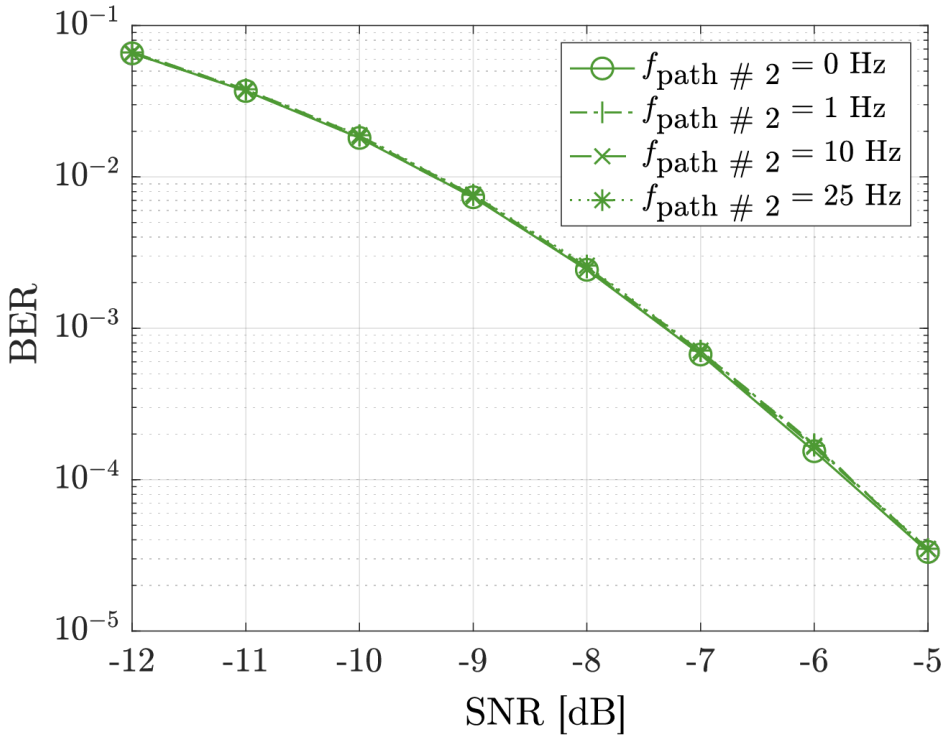

Figure 9: INL FBMC-SS waveform performance in 2 path channel with 2nd path frequency offset

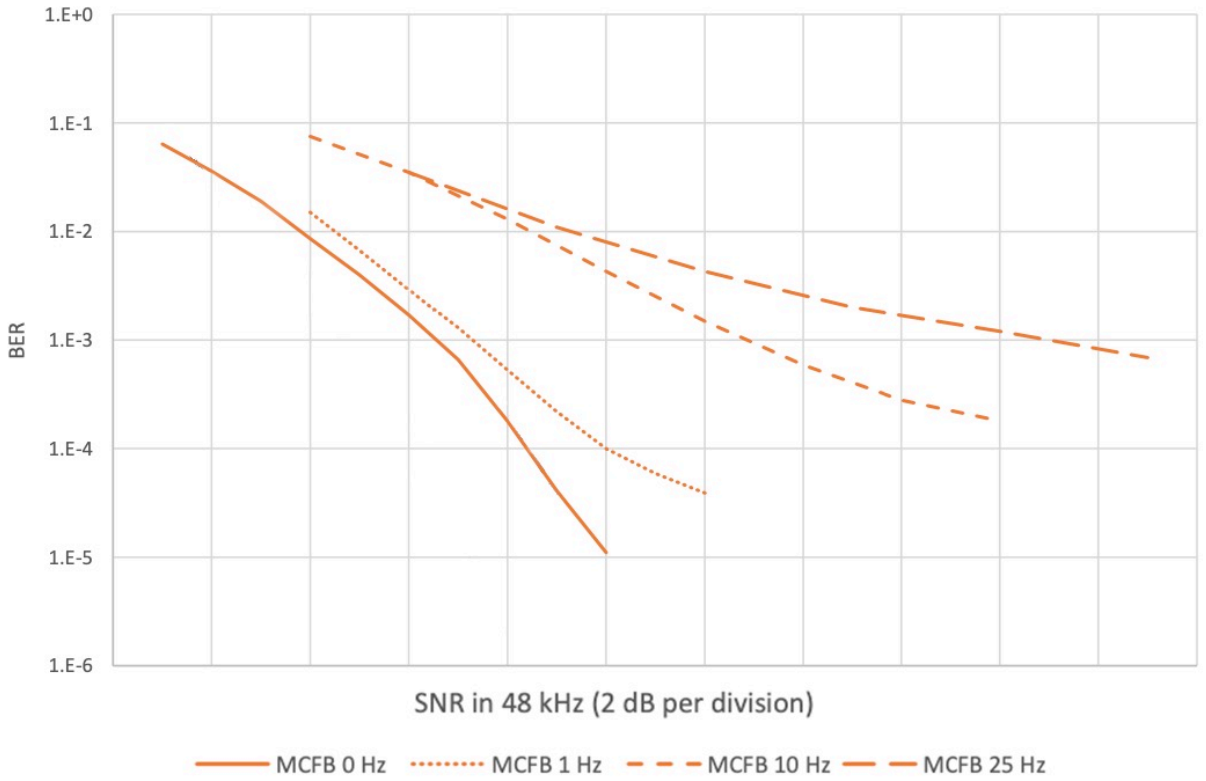

Figure 10: Nordic FBMC-SS results from [2]. Results for the Walsh waveform have been removed for clarity. Note that MCFB is interchangeable with FBMC-SS

Results for 2 path, freq. offset channel

- SNR penalty to achieve a $\mathrm{BER} = 10^{-3}$ relative to the channel $f_{\mathrm{path}\ \#2} = 0$ Hz

Table 3: Comparing results to [2]

Source of data	$f_{\mathrm{path}\ \#2} =$ 0 Hz (point A)	$f_{\mathrm{path}\ \#2} =$ 1 Hz (A to B)	$f_{\mathrm{path}\ \#2} =$ 10 Hz (A to C)	$f_{\mathrm{path}\ \#2} =$ 25 Hz (A to D)
Nordic FBMC-SS [2]	0 dB (ref. point)	0.75 dB	6.25 dB	12.5 dB

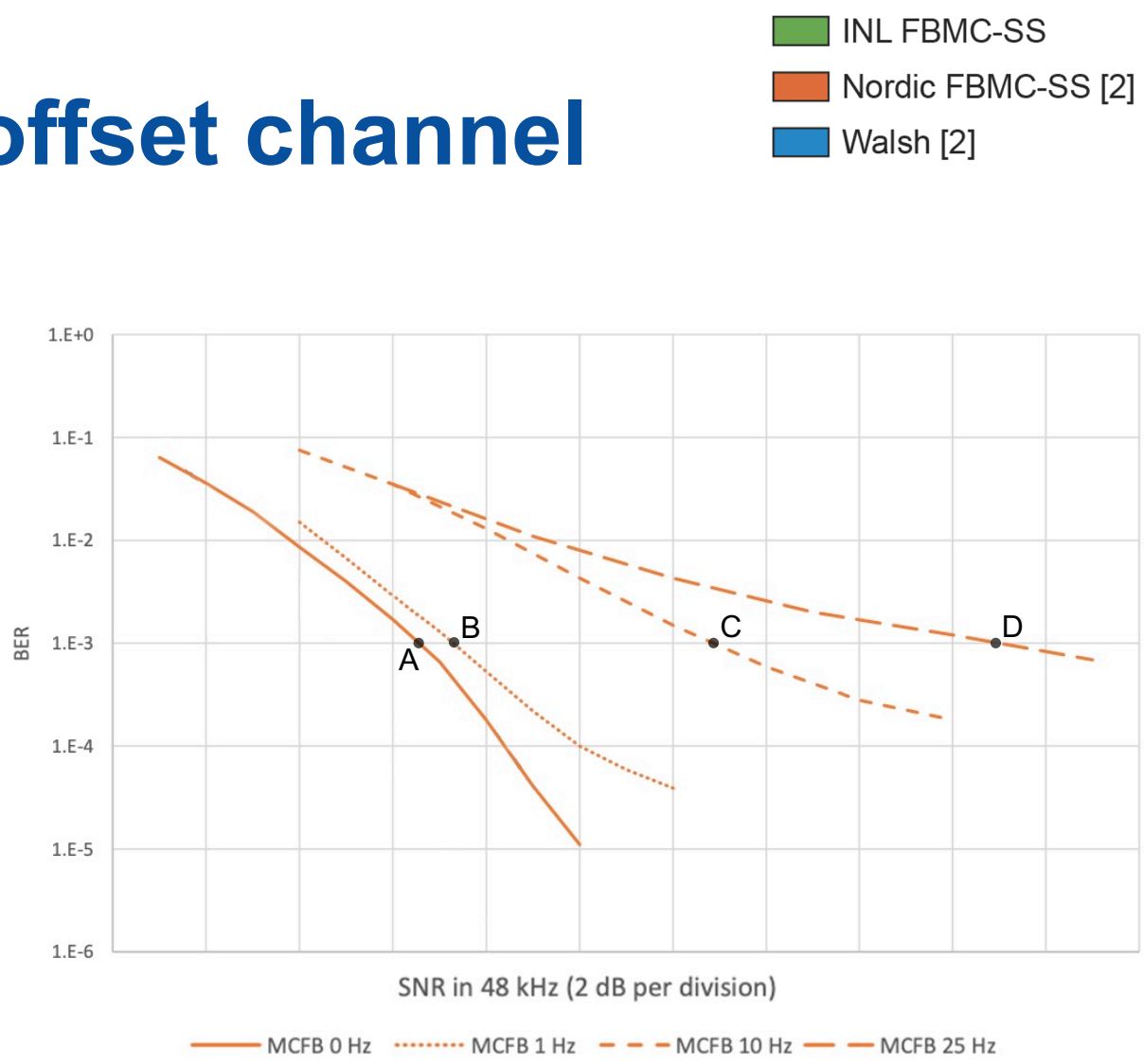

Figure 10: Nordic FBMC-SS reported in [2] with points added where $\mathrm{BER} = 10^{-3}$

Results for 2 path, freq. offset channel

- SNR penalty to achieve a $\mathrm{BER} = 10^{-3}$ relative to the channel $f_{\mathrm{path}\ \#2} = 0$ Hz

Table 3: Comparing results to [2]

Source of data	$f_{\mathrm{path}\ \#2} =$ 0 Hz (point A)	$f_{\mathrm{path}\ \#2} =$ 1 Hz (A to B)	$f_{\mathrm{path}\ \#2} =$ 10 Hz (A to C)	$f_{\mathrm{path}\ \#2} =$ 25 Hz (A to D)
Nordic FBMC-SS [2]	0 dB (ref. point)	0.75 dB	6.25 dB	12.5 dB
INL FBMC-SS	0 dB (ref. point)	0 dB	0 dB	0 dB

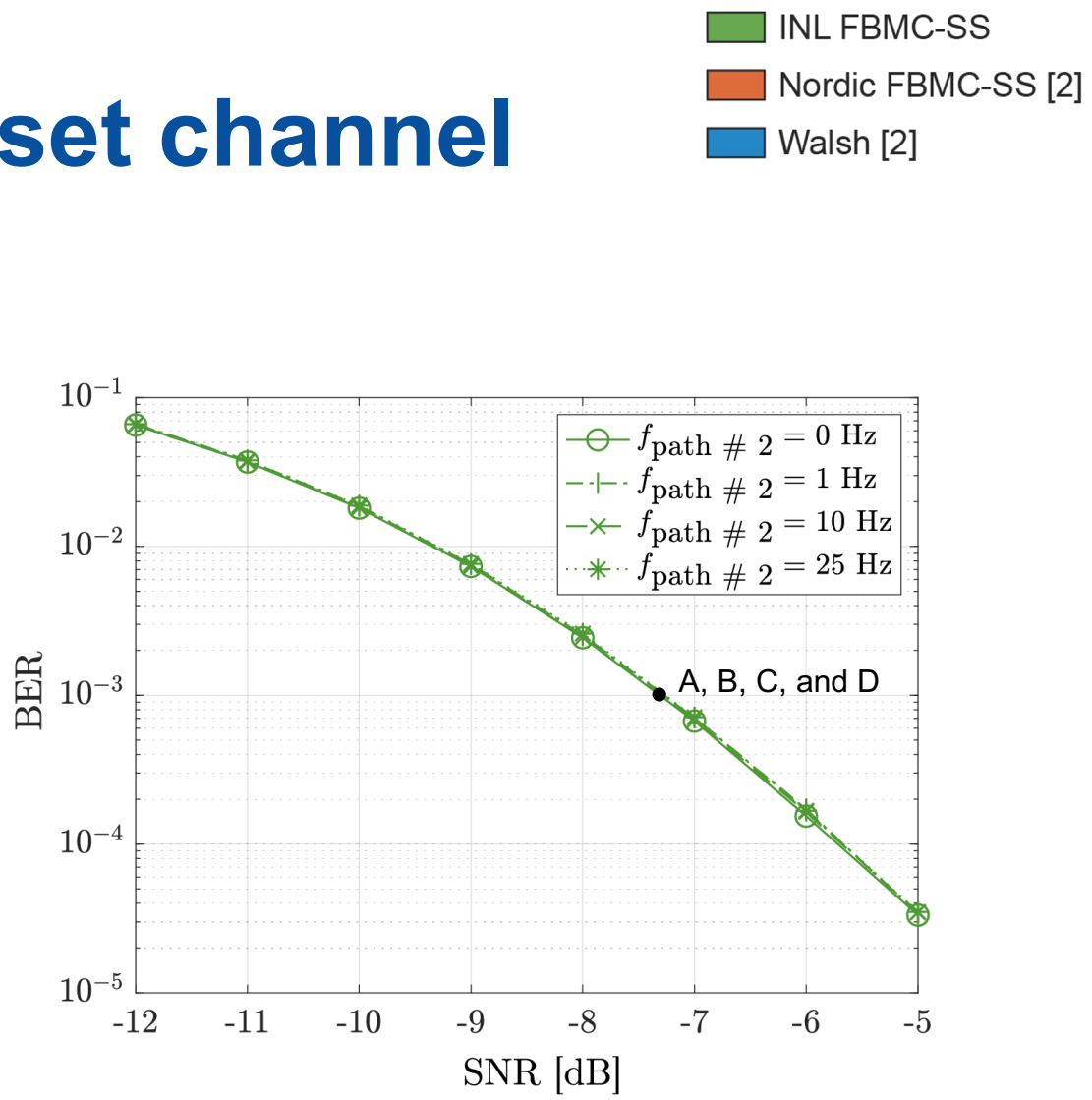

Figure 11: INL FBMC-SS results with points added where $\mathrm{BER} = 10^{-3}$

Results for 2 path, freq. offset channel

- Additional SNR required to improve BER from 10^{-2} to 10^{-3}

Table 4: Comparing marginal SNRs

Waveform	ΔSNR for $f_{\text{path \#2}} =$ 0 Hz	ΔSNR for $f_{\text{path \#2}} =$ 1 Hz	ΔSNR for $f_{\text{path \#2}} =$ 10 Hz	ΔSNR for $f_{\text{path \#2}} =$ 25 Hz
Nordic FBMC-SS [2]	2.7 dB	2.8 dB	4.4 dB	9.8 dB

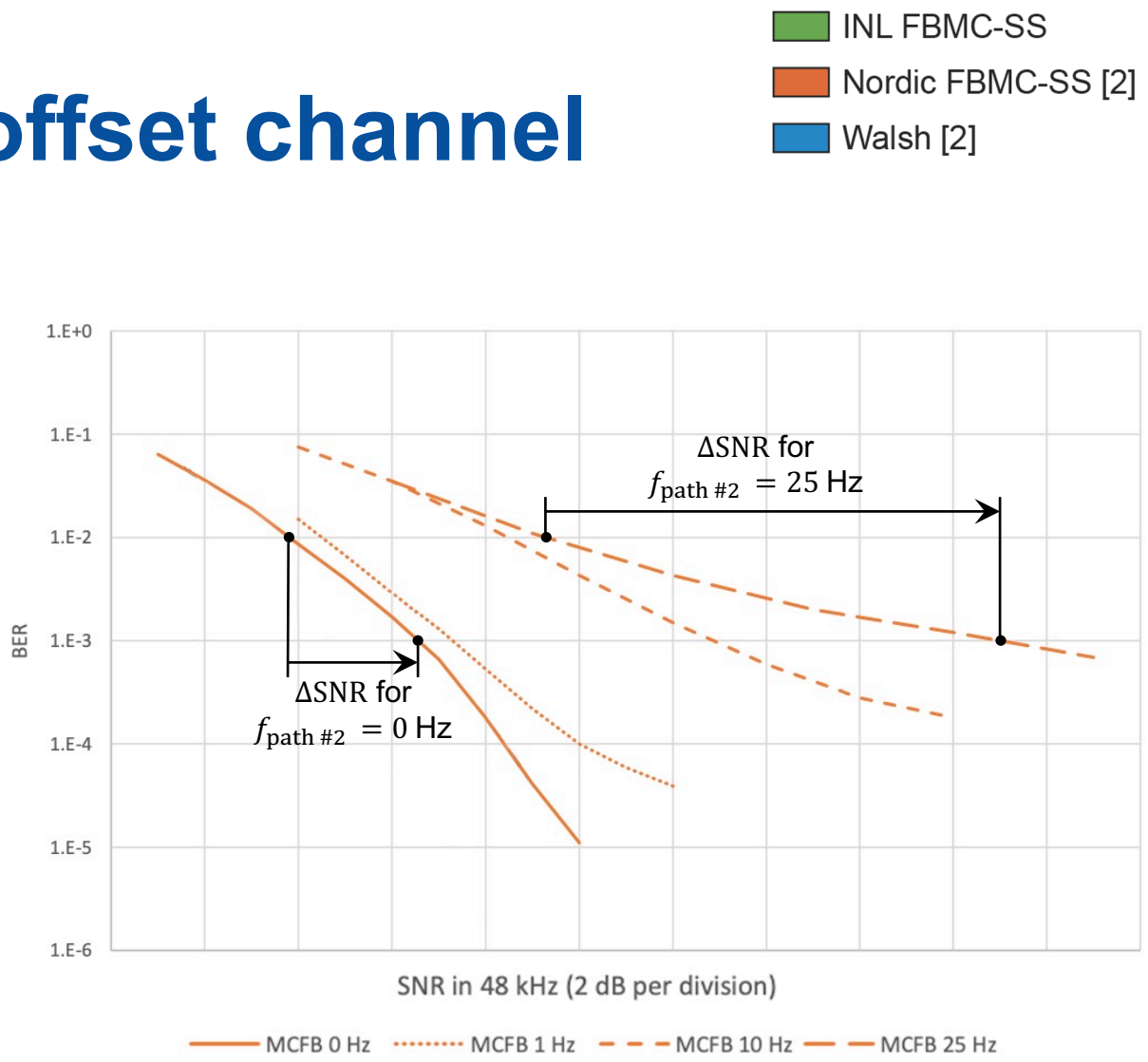

Figure 12: Nordic FBMC-SS from [2] showing the change in SNR required to improve BER from 10^{-2} to 10^{-3}

Results for 2 path, freq. offset channel

- Additional SNR required to improve BER from 10^{-2} to 10^{-3}

Table 4: Comparing marginal SNRs

Waveform	ΔSNR for $f_{\text{path \#2}} =$ 0 Hz	ΔSNR for $f_{\text{path \#2}} =$ 1 Hz	ΔSNR for $f_{\text{path \#2}} =$ 10 Hz	ΔSNR for $f_{\text{path \#2}} =$ 25 Hz
Nordic FBMC-SS [2]	2.7 dB	2.8 dB	4.4 dB	9.8 dB
INL FBMC-SS	2.1 dB	2.1 dB	2.1 dB	2.1 dB

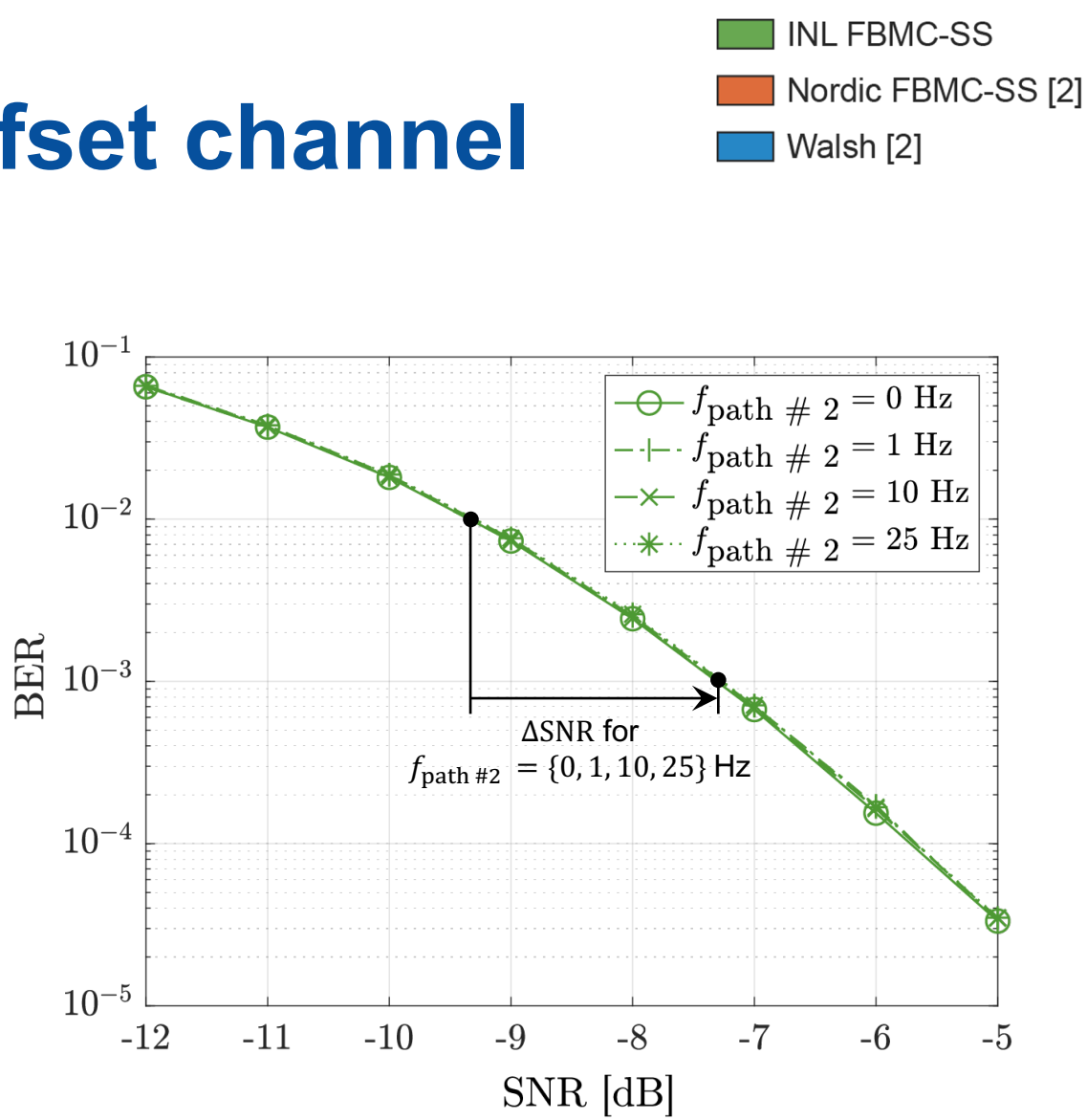

Figure 13: INL FBMC-SS results showing the change in SNR required to improve BER from 10^{-2} to 10^{-3}

Results for 2 path, freq. offset channel

INL FBMC-SS
Nordic FBMC-SS [2]
Walsh [2]

- Additional SNR required to improve BER from 10^{-2} to 10^{-3}

Table 5: Comparing marginal SNRs to Walsh performance in [2]

Waveform	ΔSNR for $f_{\text{path \#2}} =$ 0 Hz	ΔSNR for $f_{\text{path \#2}} =$ 1 Hz	ΔSNR for $f_{\text{path \#2}} =$ 10 Hz	ΔSNR for $f_{\text{path \#2}} =$ 25 Hz
Walsh reported in [2]	1.9 dB	1.9 dB	1.9 dB	2.0 dB
INL FBMC-SS	2.1 dB	2.1 dB	2.1 dB	2.1 dB

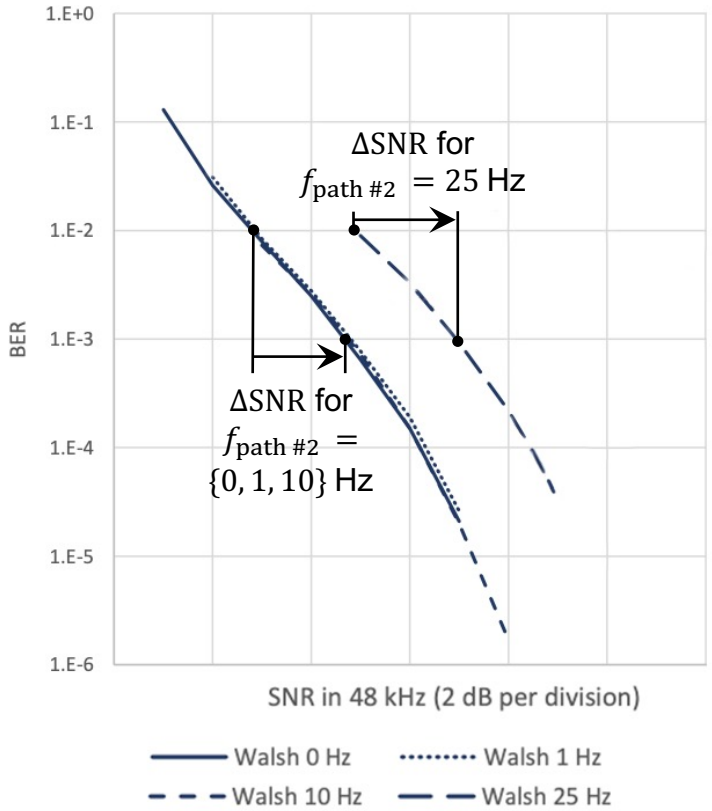

Figure 14: Walsh waveform performance reported in [2]. Lines are added depicting marginal SNR

Results for MLD and VP channels

- 2 channels with Doppler spreads are simulated
  - Mid latitude disturbed (MLD)
    - $D_s = 1$ Hz
  - Very Poor (VP)
    - $D_s = 10$ Hz

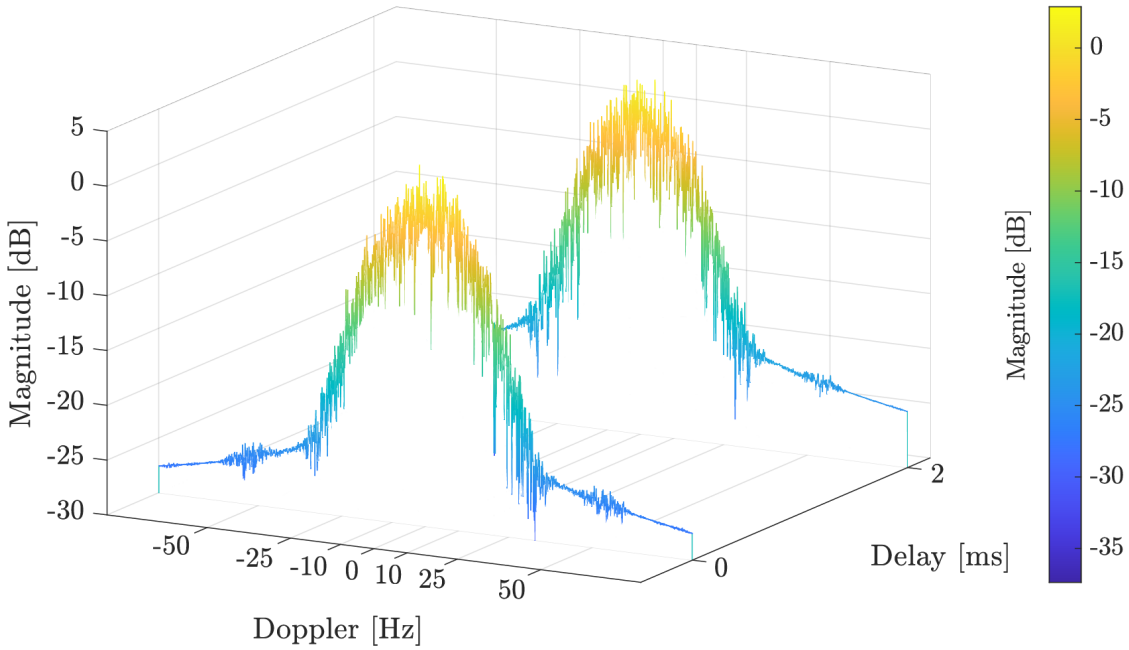

Figure 7: Delay-Doppler representation of simulated “Very Poor” (VP) channel

Results for MLD and VP channels

INL FBMC-SS
Nordic FBMC-SS [2]
Walsh [2]

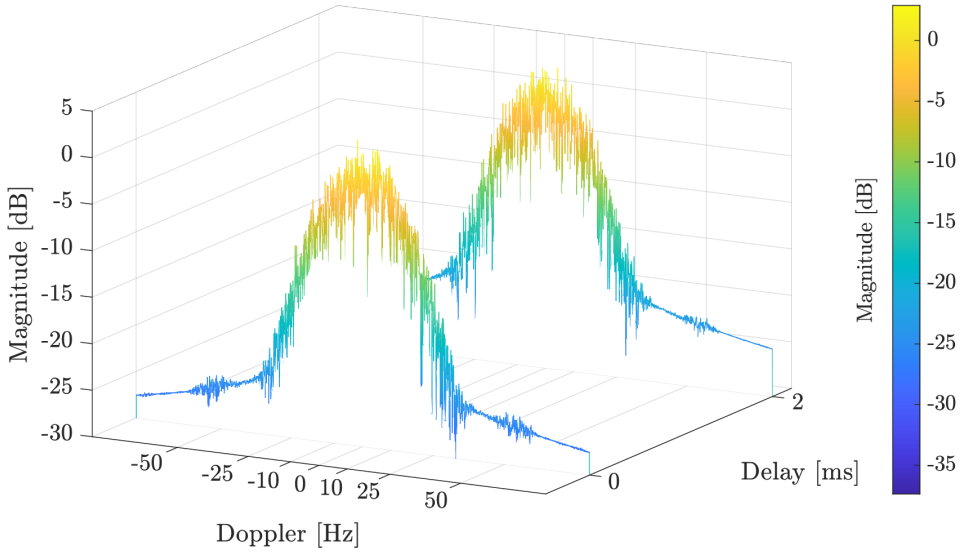

Figure 7: Delay-Doppler representation of simulated “Very Poor” (VP) channel

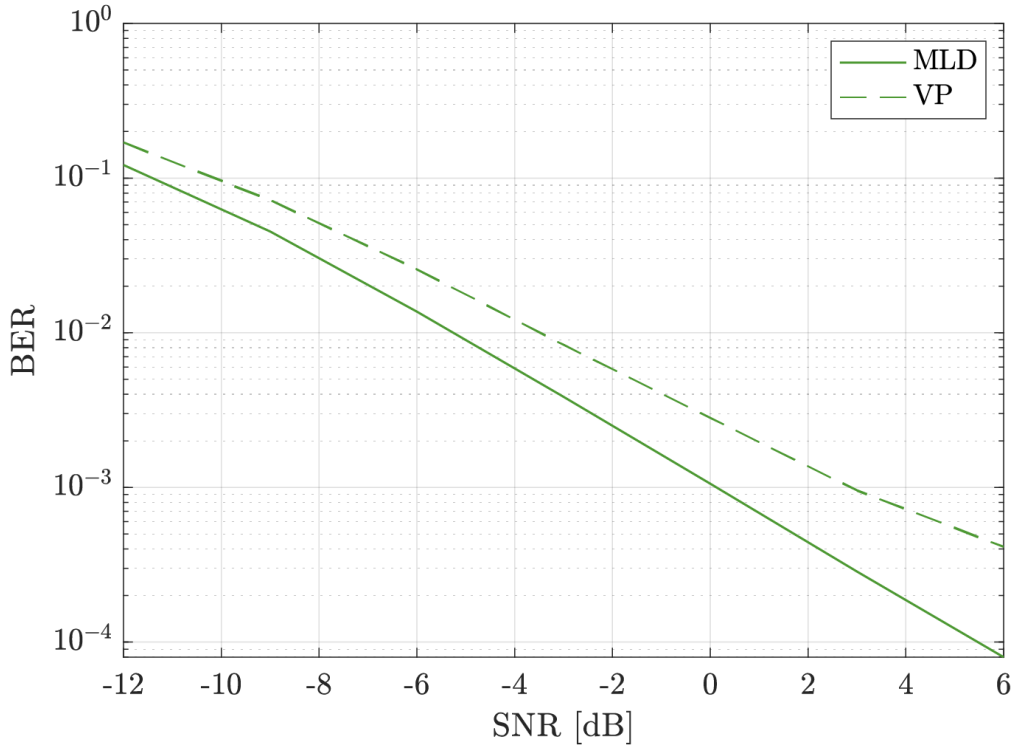

Figure 15: MLD and VP performance of INL FBMC-SS implementation

Results for MLD and VP channels

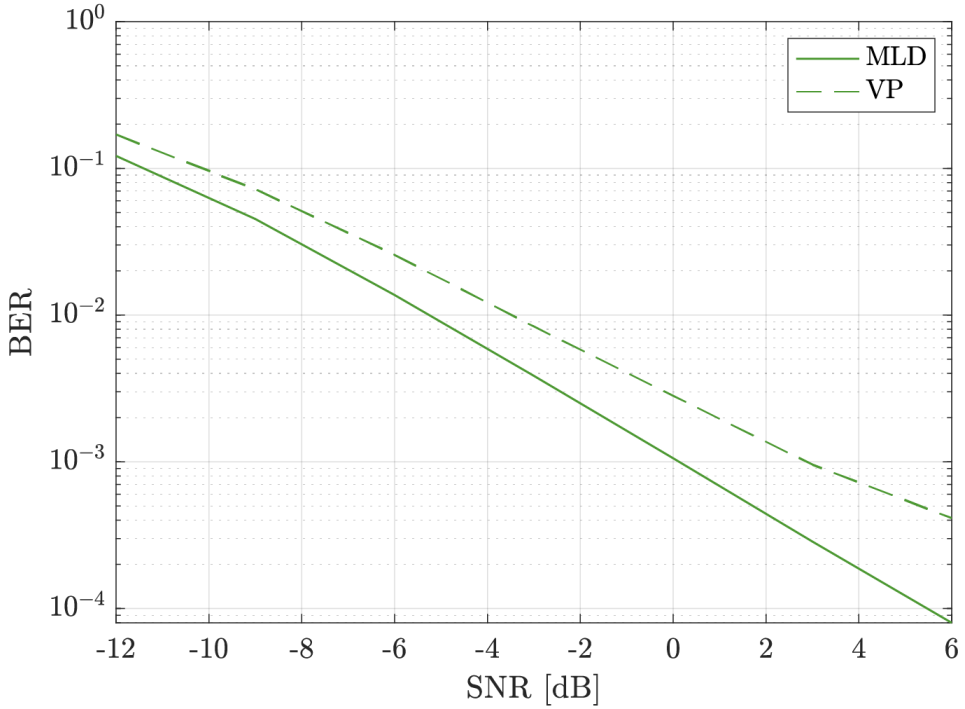

Figure 15: MLD and VP performance of INL FBMC-SS implementation

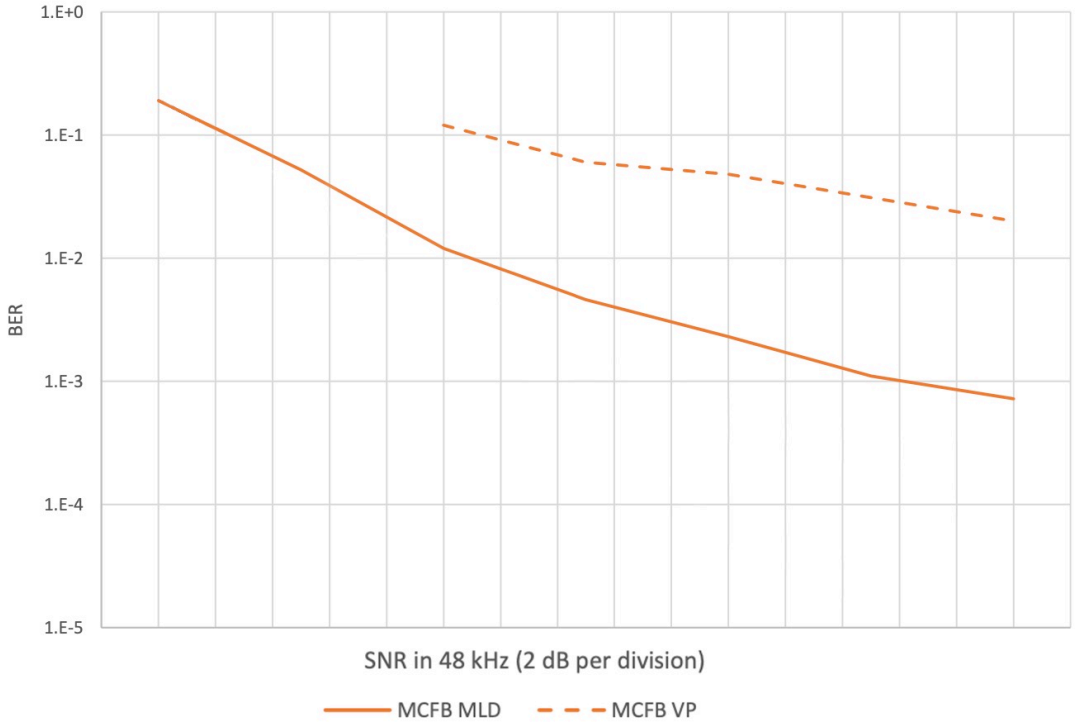

Figure 16: Nordic FBMC-SS performance for MLD and VP channels reported in [2]. Walsh results removed for clarity.

Results for MLD and VP channels

INL FBMC-SS
Nordic FBMC-SS [2]
Walsh [2]

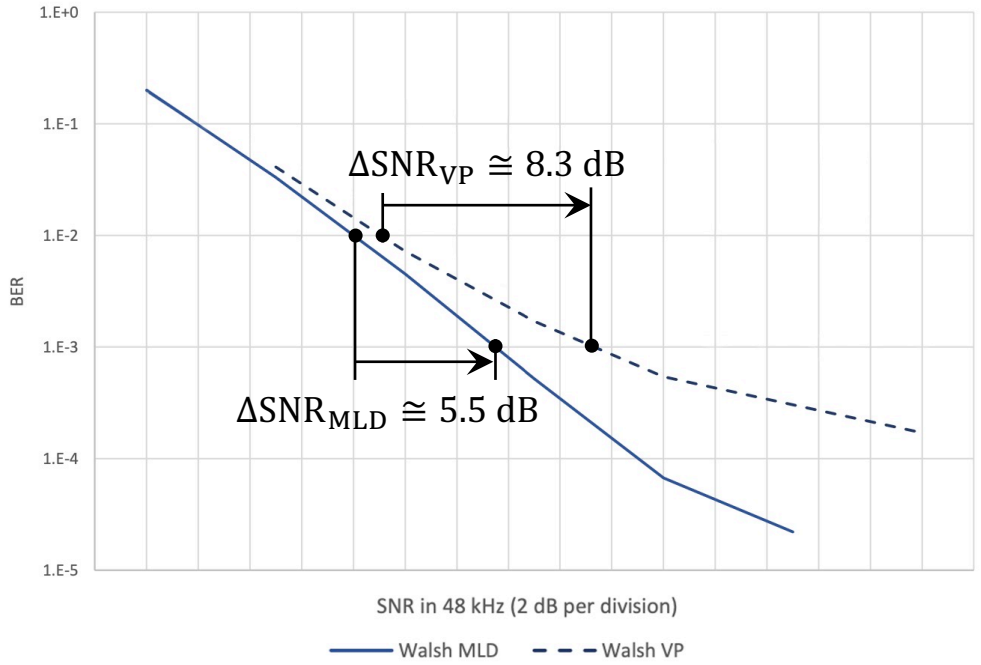

Figure 17: Additional SNR required to improve BER from 10^{-2} to 10^{-3} for Walsh reported in [2]

Table 6: Comparing results of Walsh performance to our FBMC-SS performance

Source of results	$\Delta\text{SNR}_{\text{MLD}}$, $D_s = 1$ Hz	$\Delta\text{SNR}_{\text{VP}}$, $D_s = 10$ Hz
Walsh, reported in [2]	+5.5 dB	+8.3 dB

Results for MLD and VP channels

INL FBMC-SS
Nordic FBMC-SS [2]
Walsh [2]

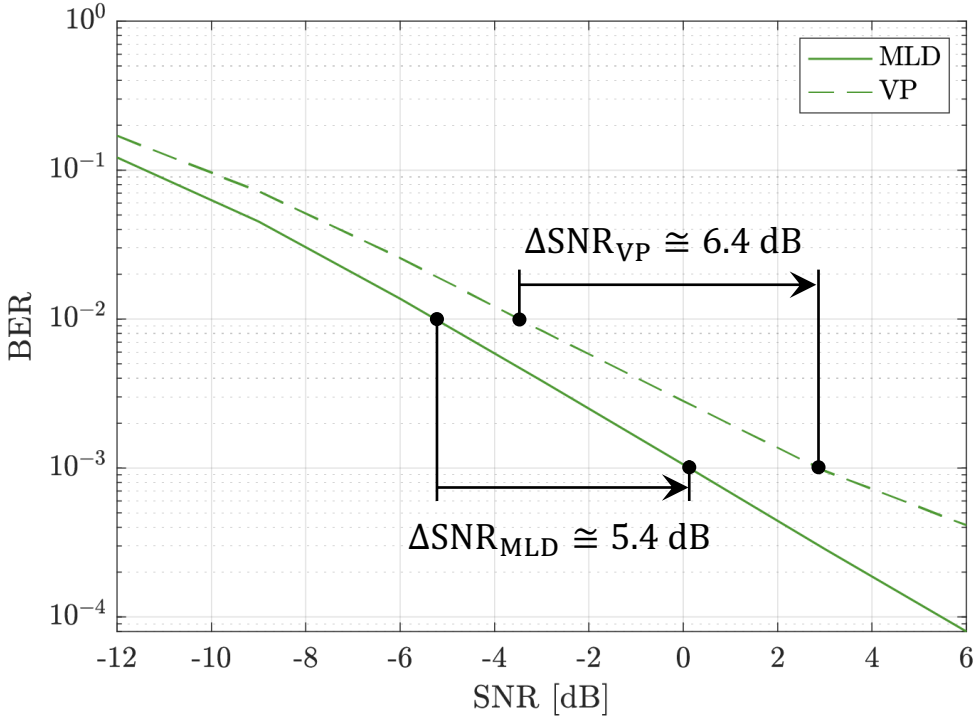

Figure 18: Additional SNR required to improve BER from 10^{-2} to 10^{-3} for INL FBMC-SS implementation

Table 6: Comparing results of Walsh performance to our FBMC-SS performance

Source of results	$\Delta\text{SNR}_{\text{MLD}}$, $D_s = 1$ Hz	$\Delta\text{SNR}_{\text{VP}}$, $D_s = 10$ Hz
Walsh reported in [2]	+5.5 dB	+8.3 dB
INL FBMC-SS	+5.4 dB	+6.4 dB

Narrowband interference test case

- AWGN channel with interferer
- Interferer has a constant power spectral density = P_{intf} dB greater than the average signal energy.
- Following results test $P_{\text{intf}} = \{-\infty, 15, 50\}$ dB

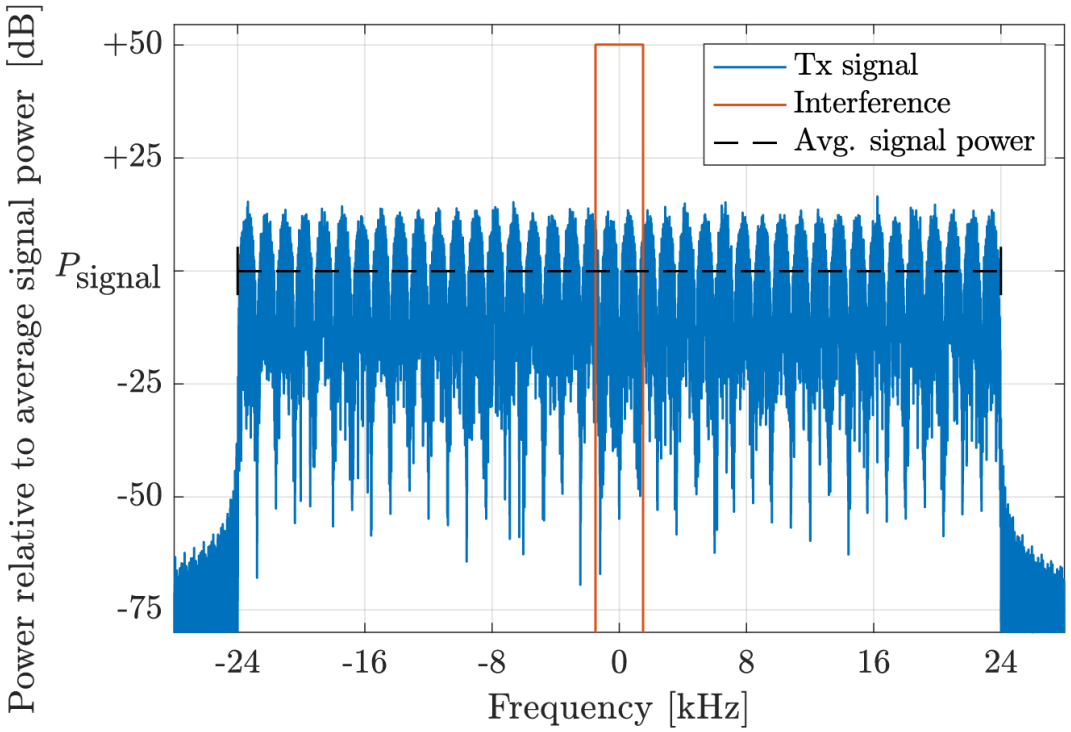

Figure 8: Depiction of interference power relative to signal in the frequency domain

Results with Narrowband interference

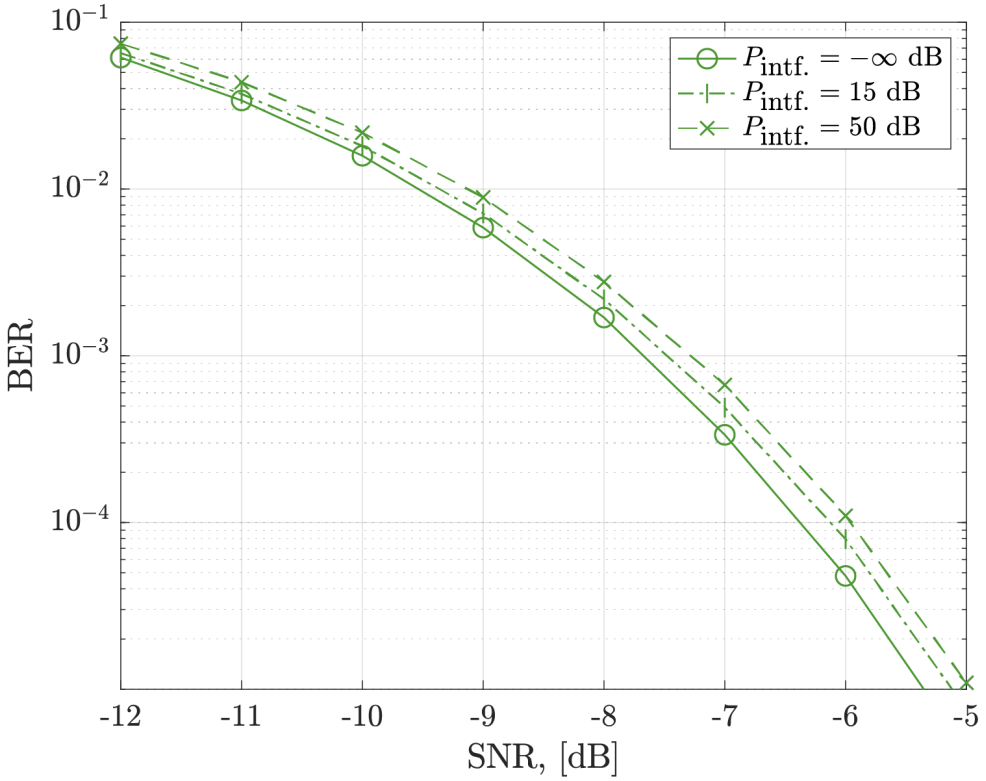

Figure 19: INL FBMC-SS performance results with varying levels of interference power

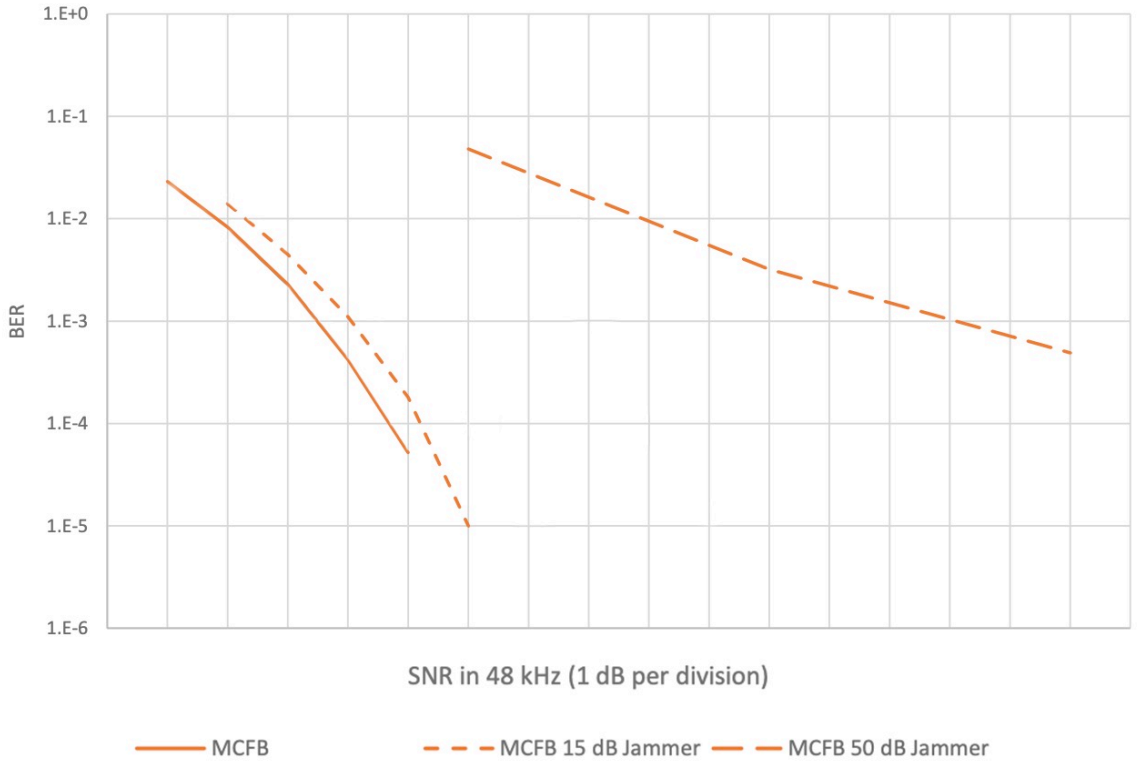

Figure 20: Nordic FBMC-SS results reported in [2] with varying levels of interference power. Walsh removed.

Results with Narrowband interference

INL FBMC-SS
Nordic FBMC-SS [2]
Walsh [2]

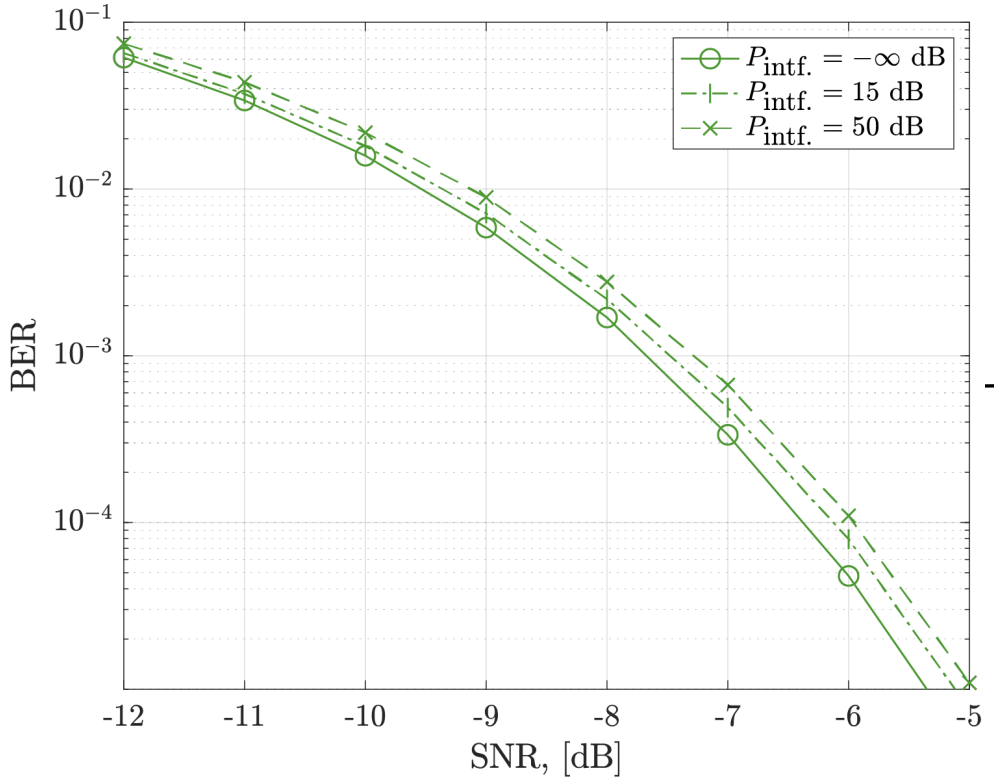

Figure 19: INL FBMC-SS performance results with varying levels of interference power

→ The NMF operation greatly reduces the impact of interference

Comparing results by matching AWGN

INL FBMC-SS
Nordic FBMC-SS [2]
Walsh [2]

- To compare with the Walsh reported in [2], the plots can be overlaid

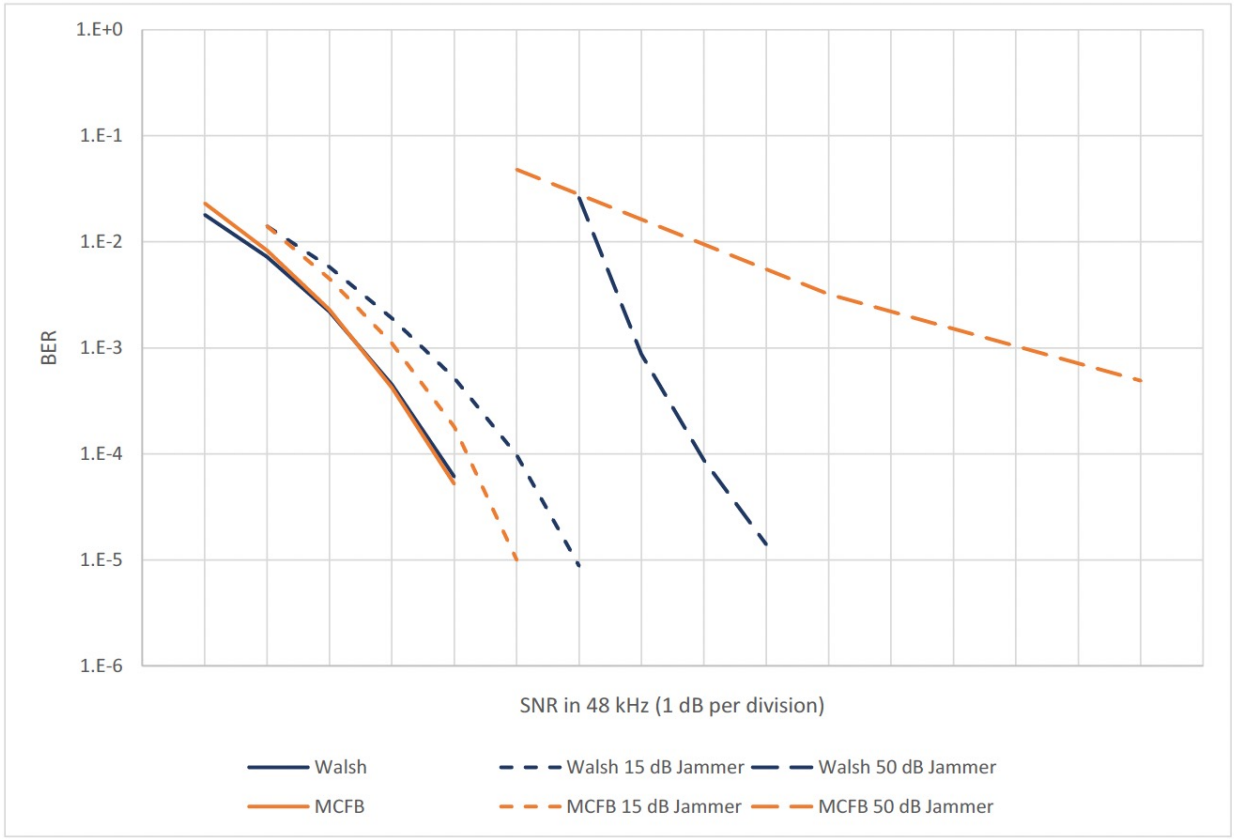

Figure 21: Performance results of Walsh and Nordic FBMC-SS presented in [2]

Comparing results by matching AWGN

INL FBMC-SS
Nordic FBMC-SS [2]
Walsh [2]

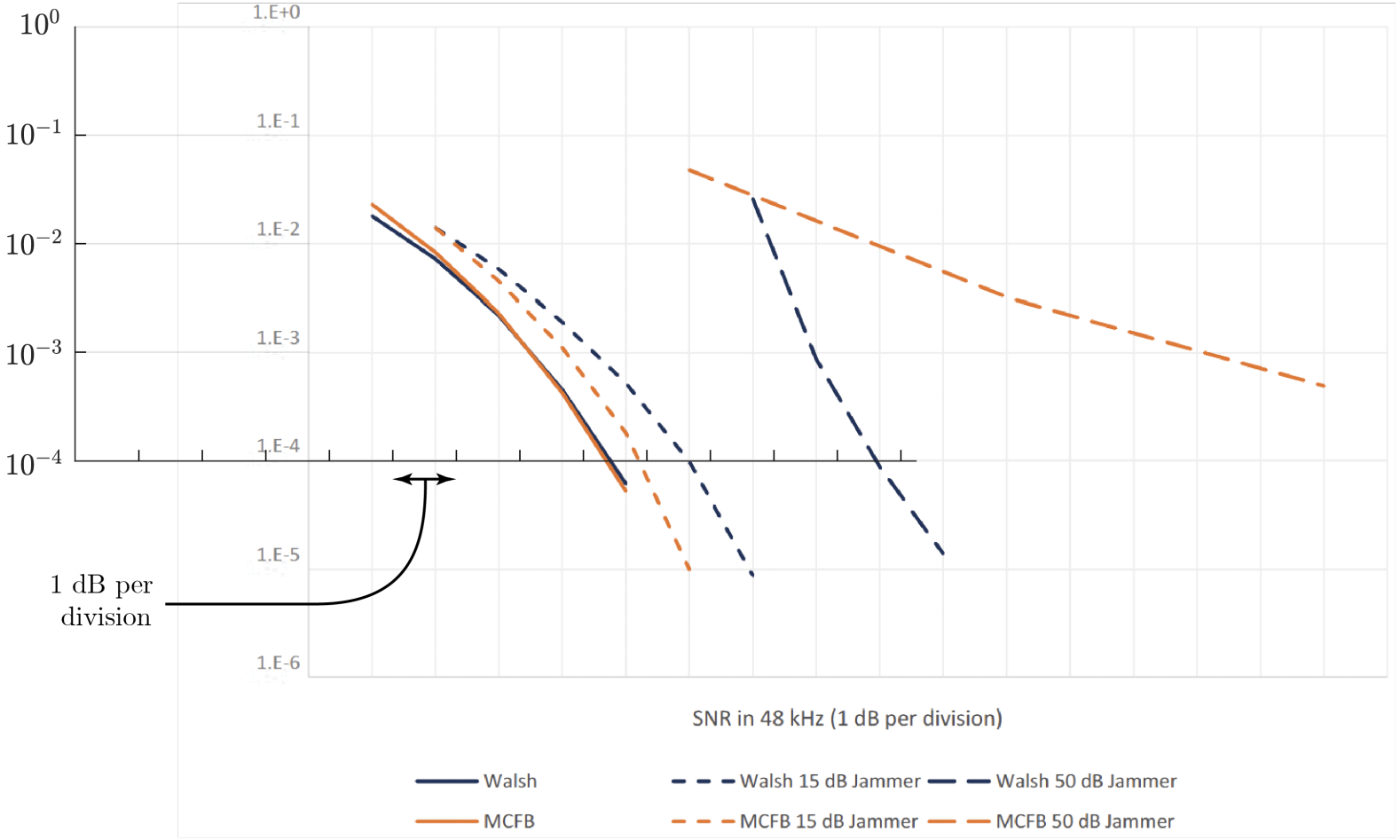

Figure 22: Fit our axes to figure 4 in [2]

Comparing results by matching AWGN

INL FBMC-SS
Nordic FBMC-SS [2]
Walsh [2]

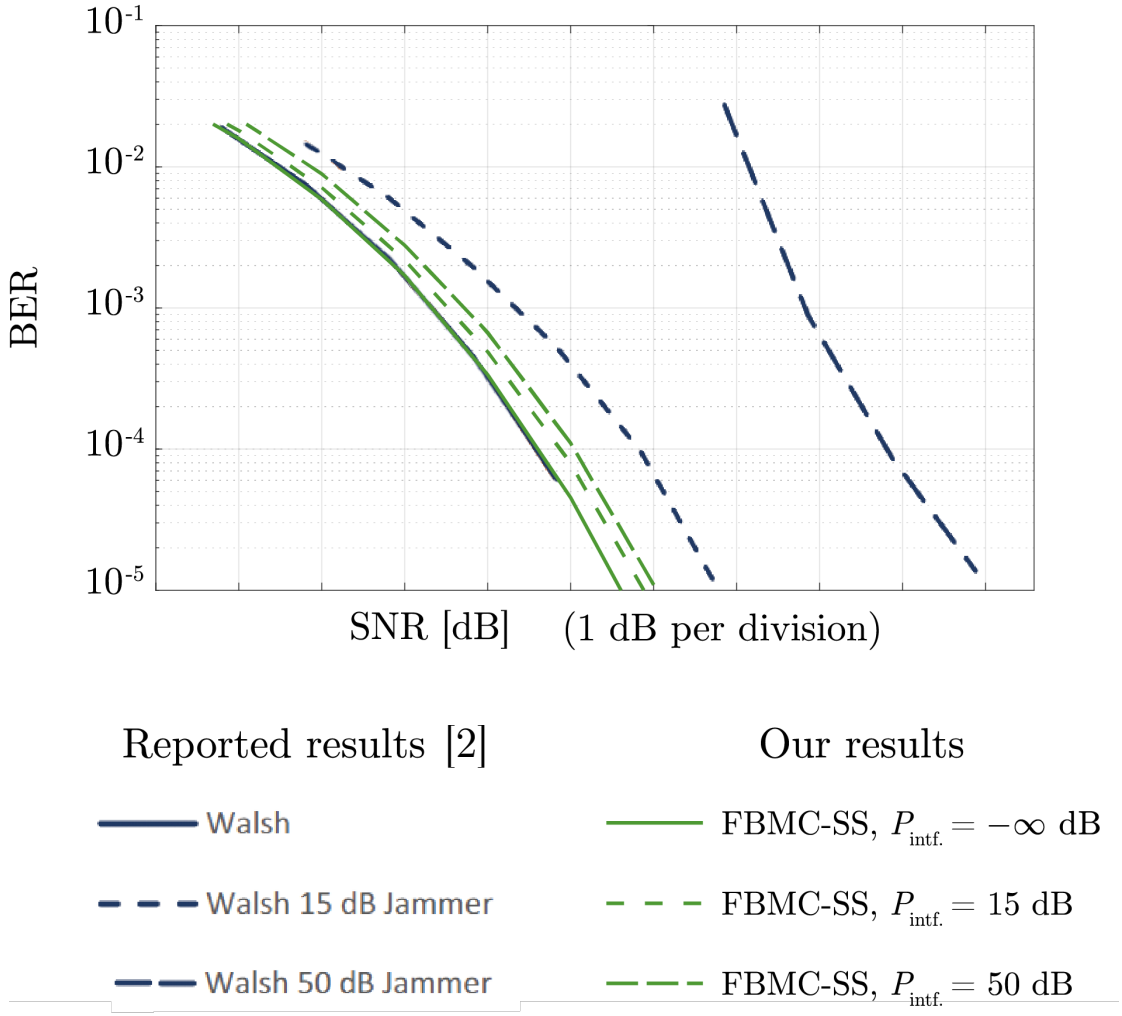

Figure 23: Walsh performance reported in [2] compared against our INL FBMC-SS performance in the presence of narrowband interference

Comparing results by matching AWGN

INL FBMC-SS
Nordic FBMC-SS [2]
Walsh [2]

Table 7: SNR loss at BER = 10^{-3} as power of narrowband interference increases

Interference Power Level	Walsh results from [2]	INL FBMC-SS results
$-\infty$ dB	Reference	Reference
15 dB	+1 dB	+0.2 dB
50 dB	+4.5 dB	+0.4 dB

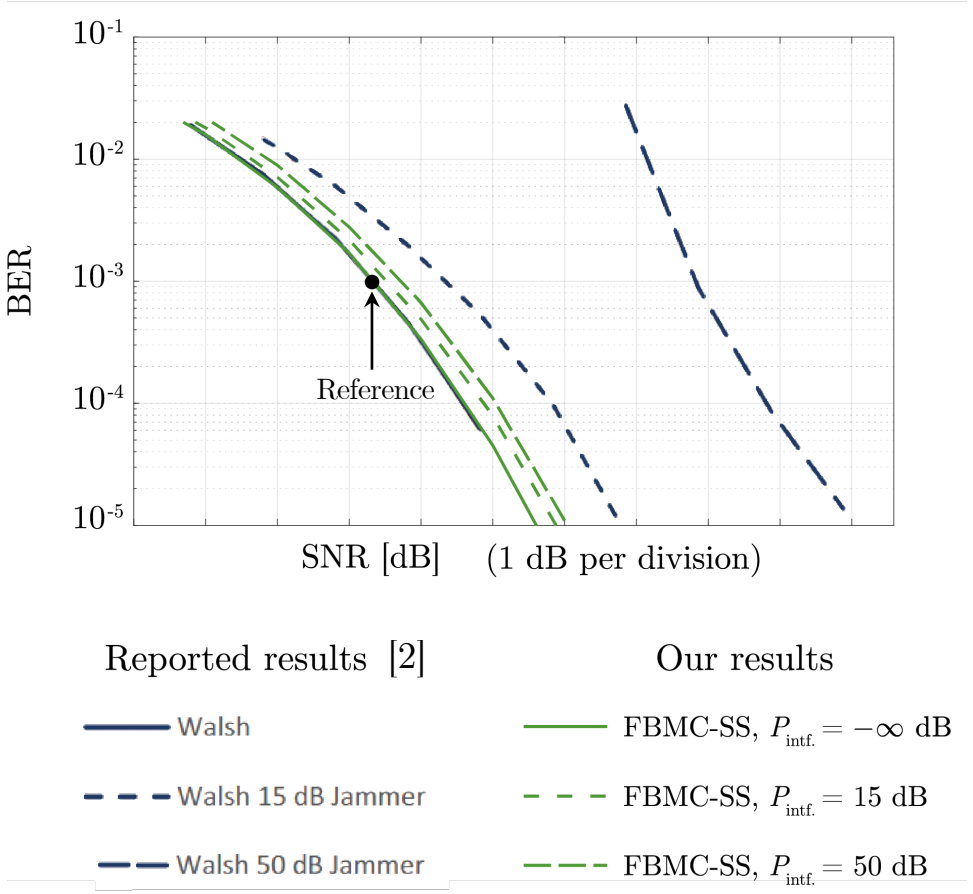

Figure 24: Walsh performance reported in [3] compared against our INL FBMC-SS implementation in the presence of narrowband interference

Multiple narrowband interferers

- 2 cases with multiple narrowband interferers:
  1. 4, 3 kHz interferers placed randomly and nonoverlapping in passband
  2. 8, 3 kHz interferers placed randomly and nonoverlapping in passband
- $P_{\text{intf}} = 50$ dB for each interferer

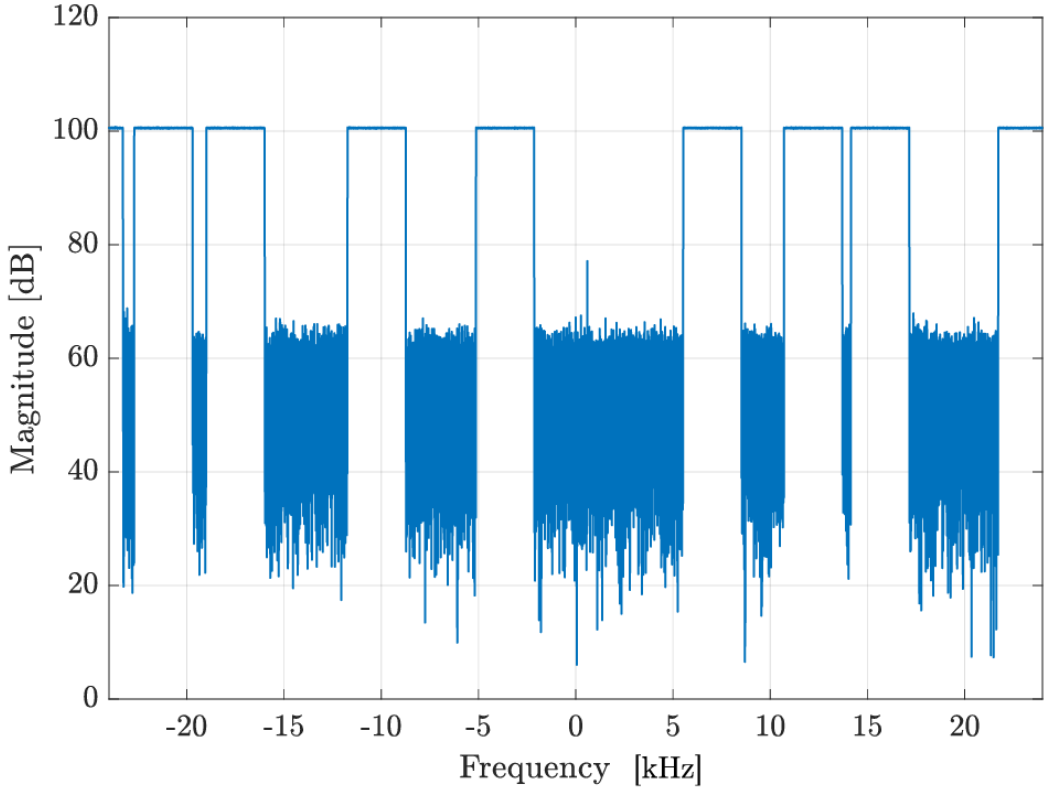

Figure 25: Received FBMC-SS signal polluted with 8 3 kHz wide interferers over signal passband at $\text{SNR} = -10$ dB

Multiple narrowband interferers

- In AWGN channels, the loss is bounded is bounded by:

$$\Delta\text{SNR} \leq 10\log_{10}\left(\left(\left\lceil\frac{W_{\text{intf}}}{W_{\text{sub}}}\right\rceil + 1\right) \times W_{\text{sub}}/W_{\text{sig}}\right)$$

  - Loss due to reduced processing gain from reweighted subcarriers
- For these cases, loss is bounded by:
  - $\Delta\text{SNR}_{8\text{ intfs.}} \leq 6.99$ dB
  - $\Delta\text{SNR}_{4\text{ intfs.}} \leq 2.22$ dB

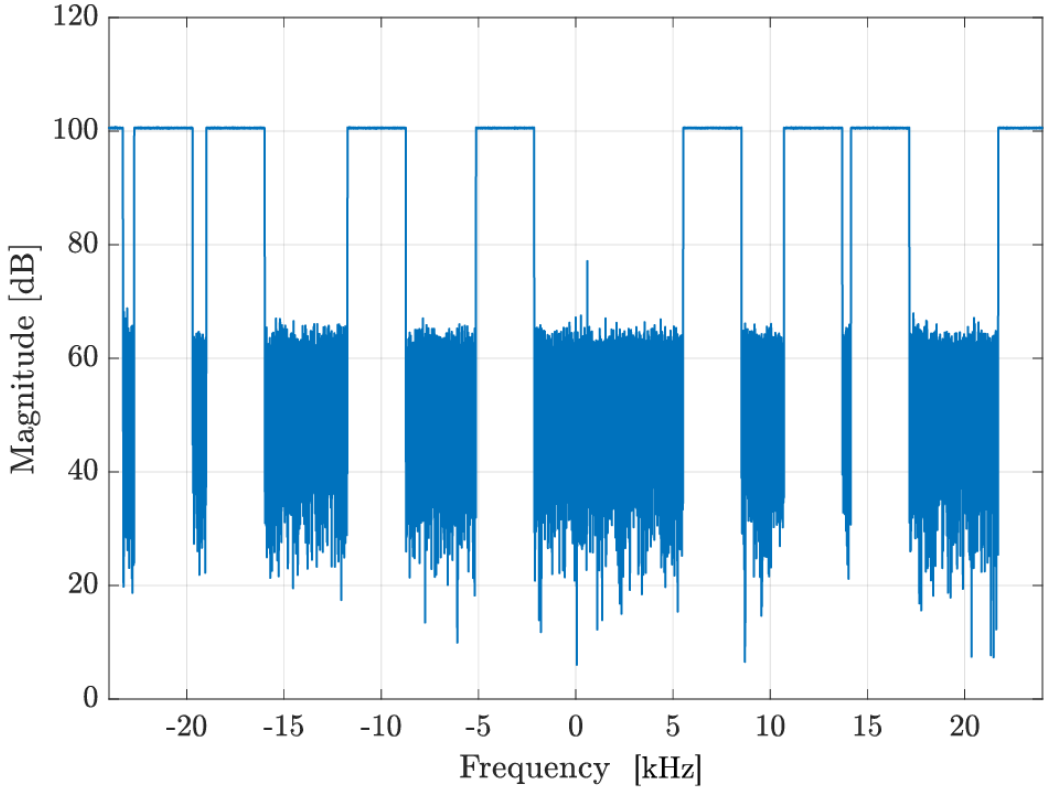

Figure 25: Received FBMC-SS signal polluted with 8 3 kHz wide interferers over signal passband at $\text{SNR} = -10$ dB

Multiple narrowband interferers

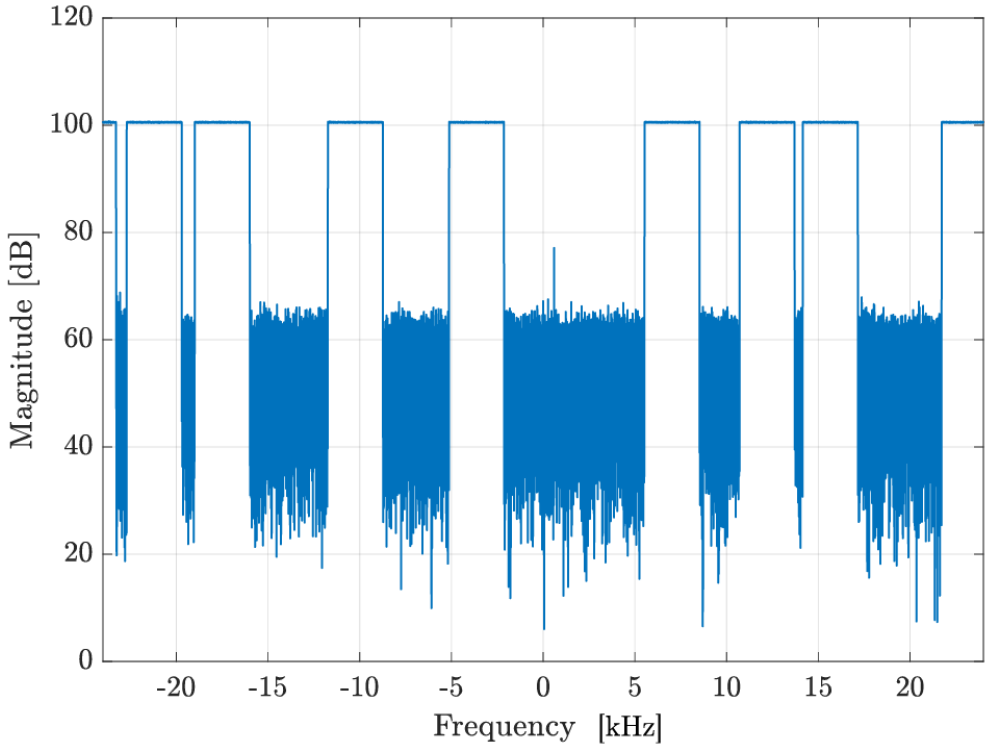

Figure 25: Received FBMC-SS signal polluted with 8 3 kHz wide interferers over signal passband at $\mathrm{SNR} = -10$ dB

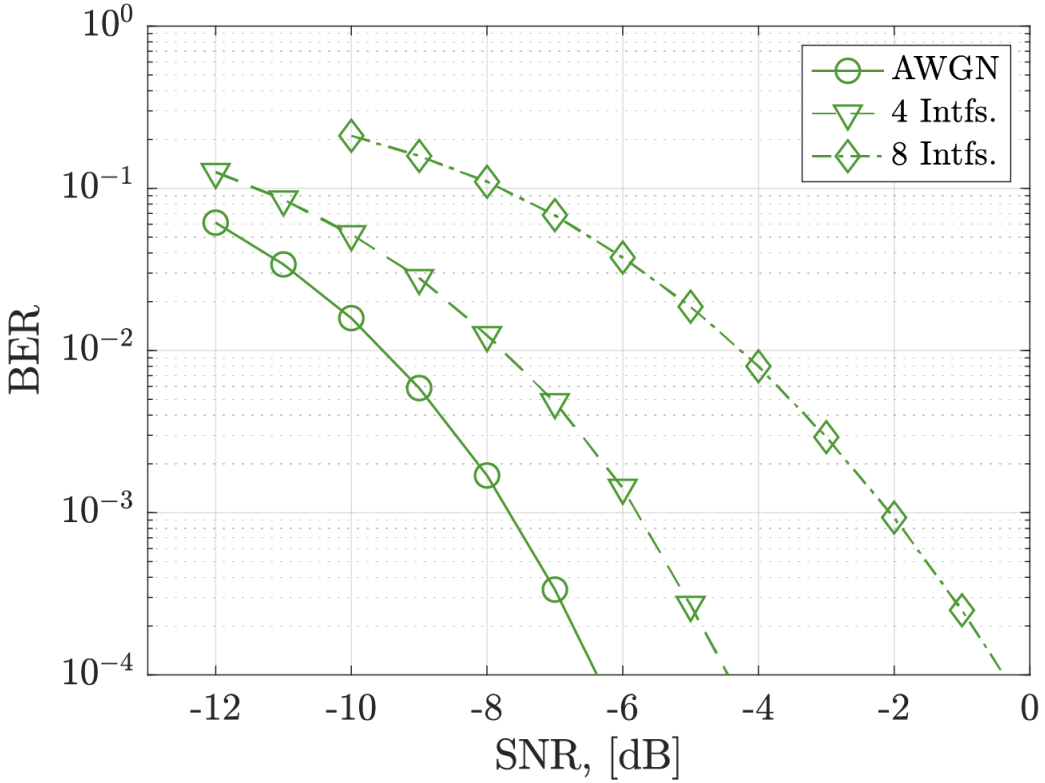

Figure 26: BER performance of INL FBMC-SS implementation in both interference cases

Multiple narrowband interferers

- For these cases, loss is bounded by:
  - $\Delta\mathrm{SNR}_{8\ \mathrm{intfs.}} \leq 6.99$ dB
  - $\Delta\mathrm{SNR}_{4\ \mathrm{intfs.}} \leq 2.22$ dB
- Observed loss at $\mathrm{BER} = 10^{-2}$:
  - $\Delta\mathrm{SNR}_{8\ \mathrm{intfs.}} = 5.28$ dB
  - $\Delta\mathrm{SNR}_{4\ \mathrm{intfs.}} = 1.77$ dB

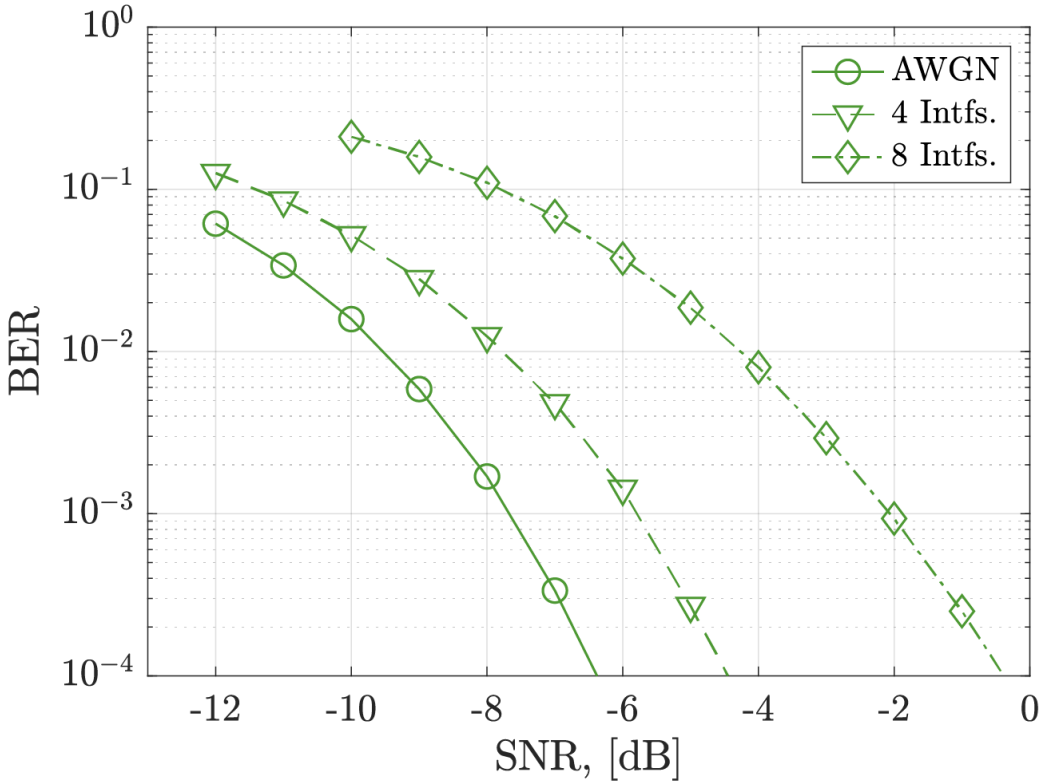

Figure 26: BER performance of INL FBMC-SS implementation in both interference cases

Swept tone interference

- A single tone with $P_{\text{tone}} = 50$ dB
- Tone sweeps in frequency at rate of:
  1. 3 kHz in 20 seconds (150 Hz/sec)
  2. 12 kHz in half of packet interval (~21.2 kHz/sec)

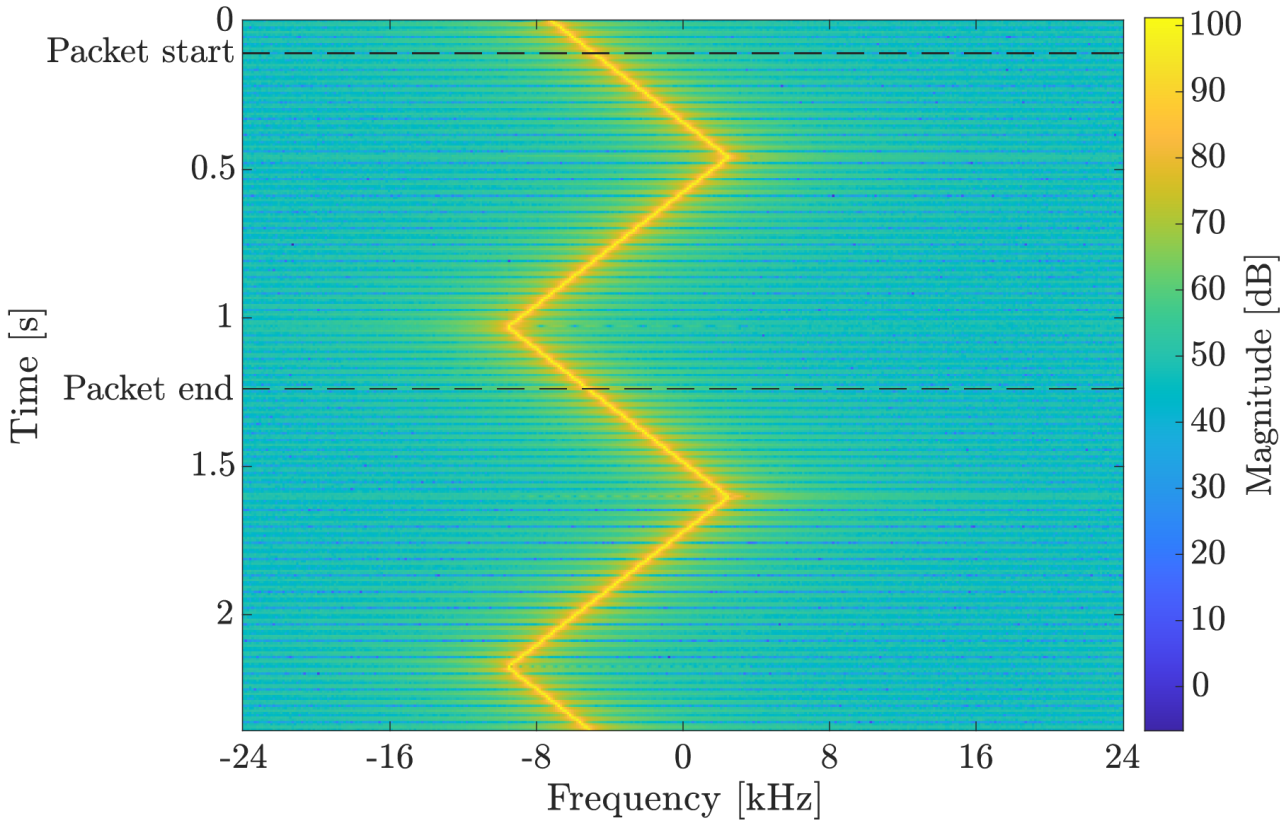

Figure 27: Spectrogram of received FBMC-SS signal polluted with an interferer swept at rate of 21.2 kHz/sec

Swept tone interference

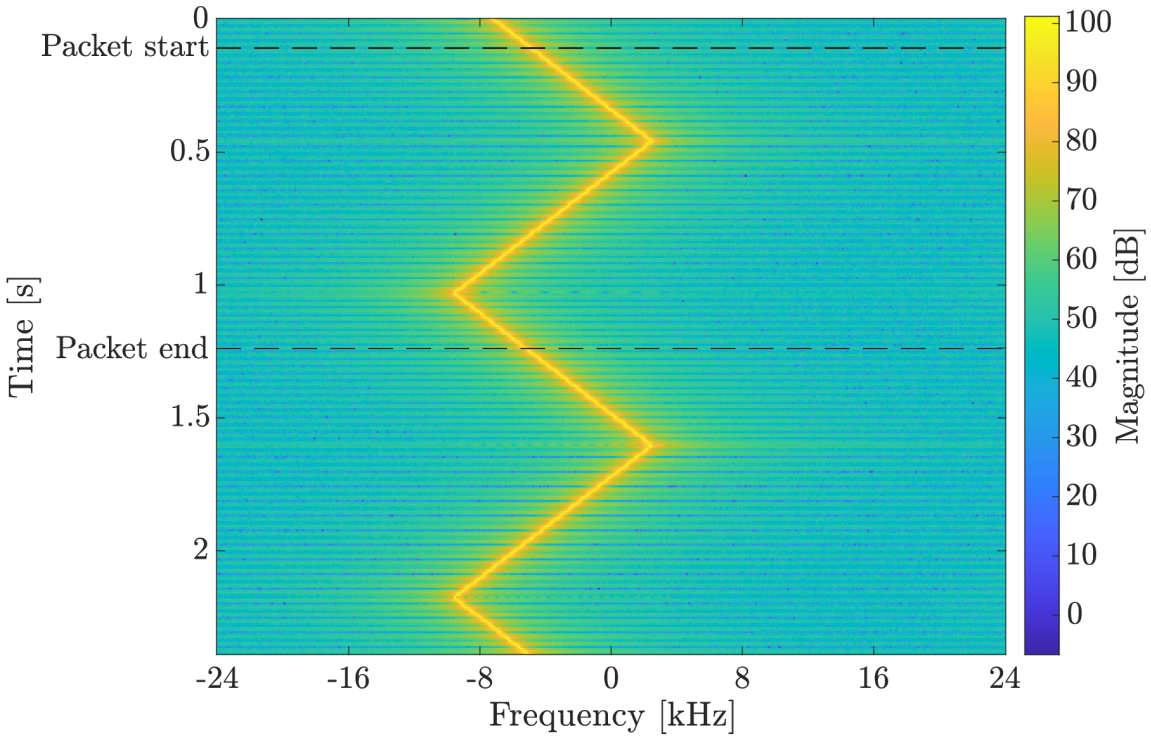

Figure 27: Spectrogram of received FBMC-SS signal polluted with an interferer swept at rate of 21.2 kHz/sec

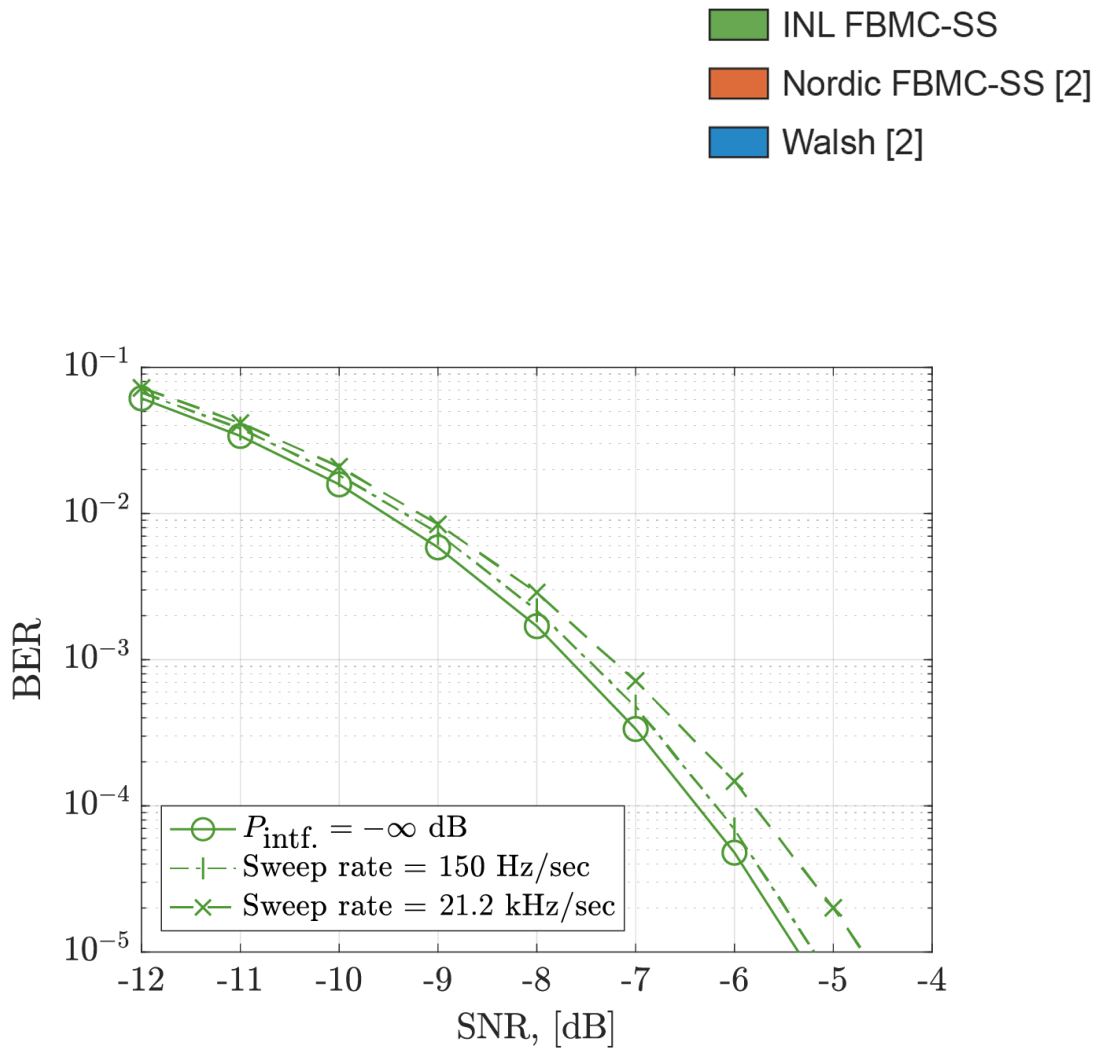

Figure 28: BER performance of INL FBMC-SS implementation in the presence of a high-power swept interferer

Conclusion

- FBMC-SS receiver can be designed to effectively handle:
  - 2-path channels with $T_{\text{mode}} = 2$ ms and significant f_{CFO}
  - 2-path HF channels with $T_{\text{mode}} = 2$ ms and $D_s = \{1, 10\}$ Hz
  - High powered interference, $P_{\text{intf}} = 50$ dB
- Further, FBMC-SS can be effectively recovered when the propagation channel contains:
  - Significant congestion from other users
  - Highly-dynamic interference
  - This performance is an intrinsic feature of the FBMC-SS structure
- All results generated using a transceiver pair provided with no information about any impairments present in channel

Appendix A: Freq. offset channel

INL FBMC-SS
Nordic FBMC-SS [2]
Walsh [2]

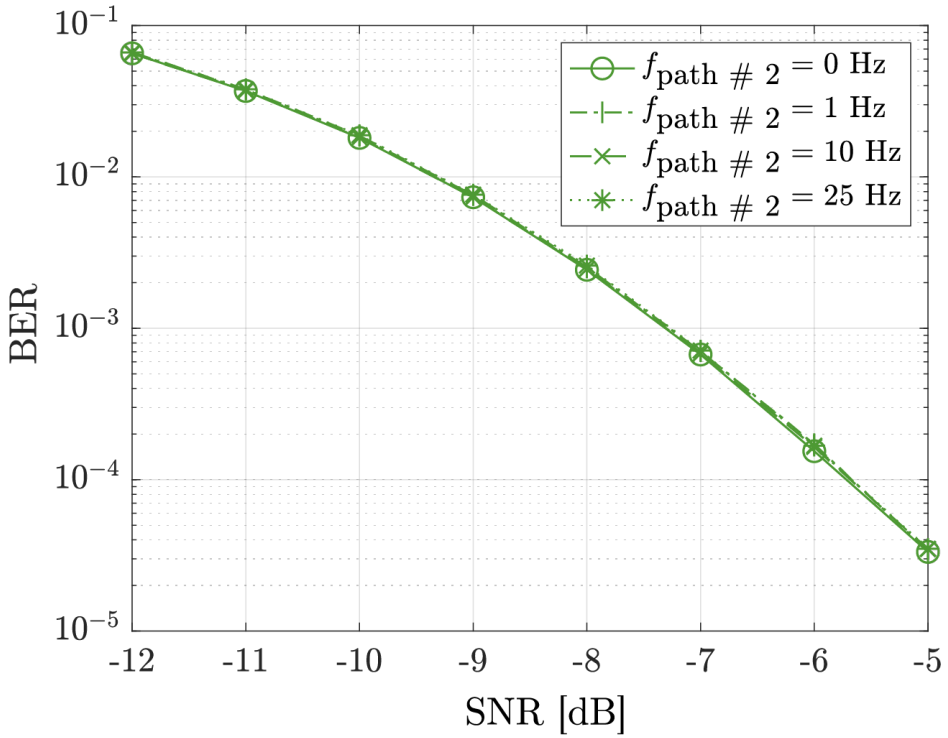

Figure A1: INL FBMC-SS implementation performance in 2 path channel with 2nd path frequency offset

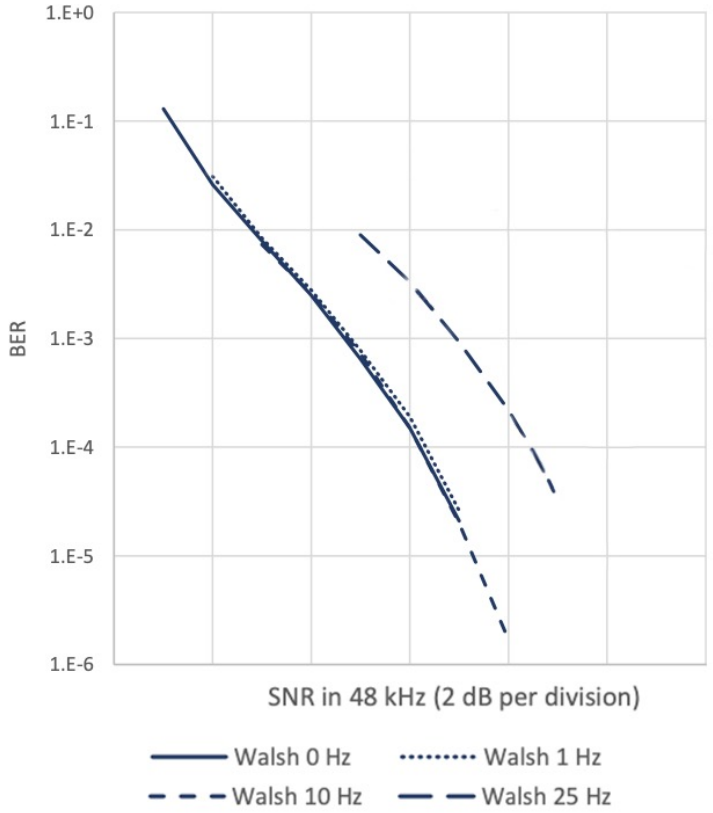

Figure A2: Reported Walsh results from [2]

Appendix B: fitting in AWGN

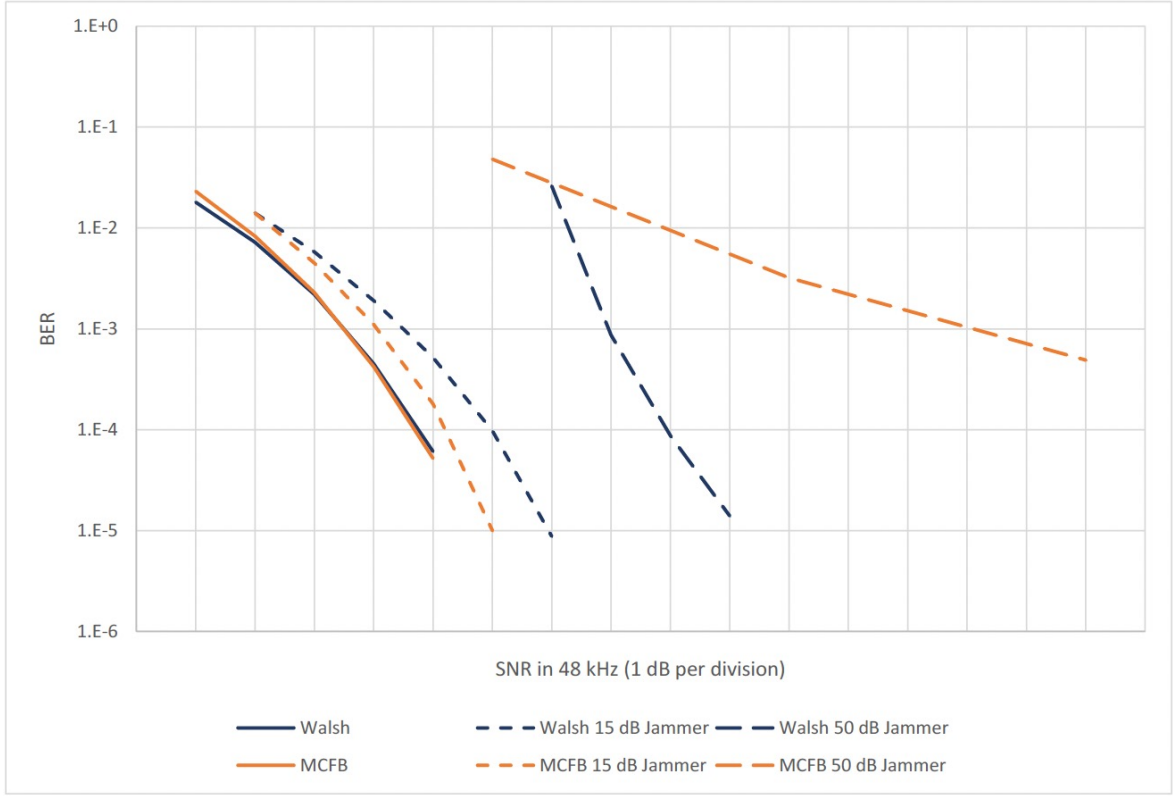

Figure B1: 48 kHz waveform comparisons in AWGN with varying levels of interference

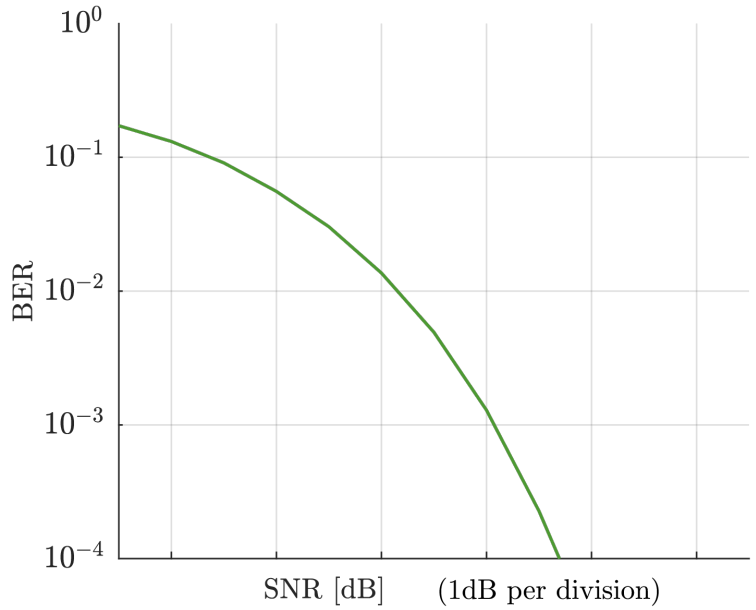

Figure B2: Performance of our implementation in AWGN

Appendix B: fitting in AWGN (cont.)

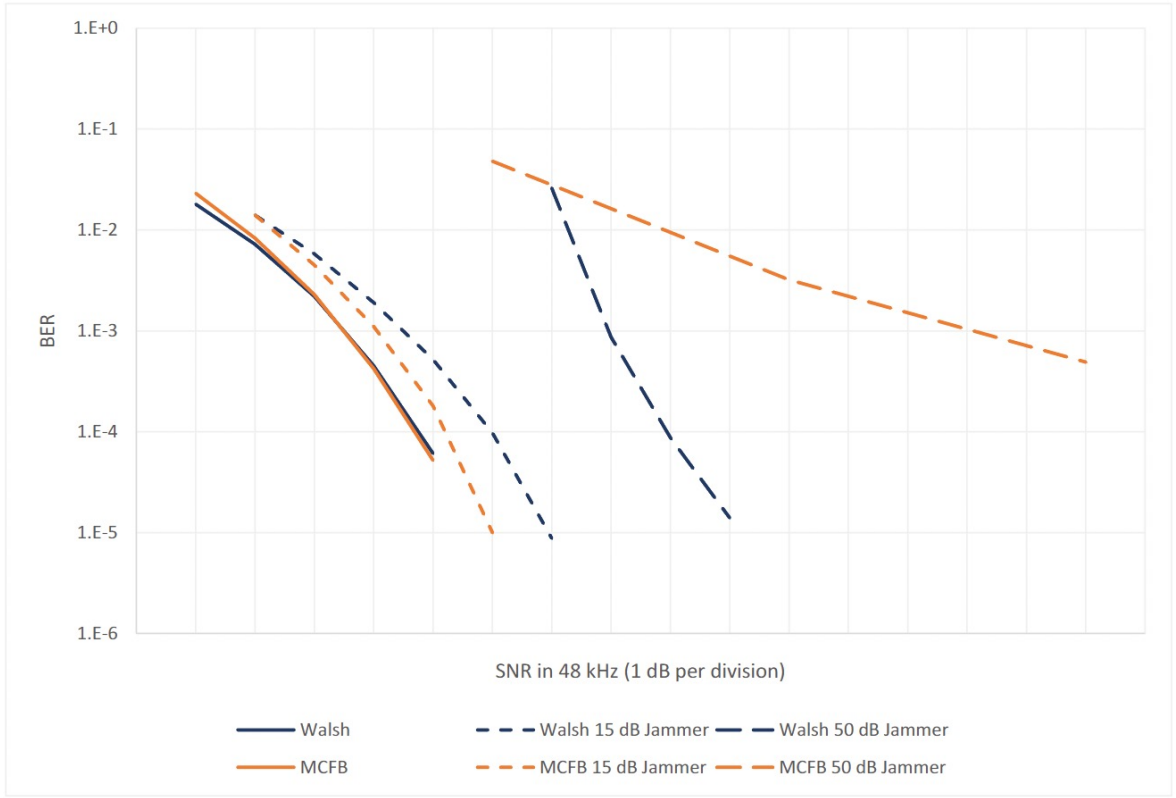

Figure B1: 48 kHz waveform comparisons in AWGN with varying levels of interference

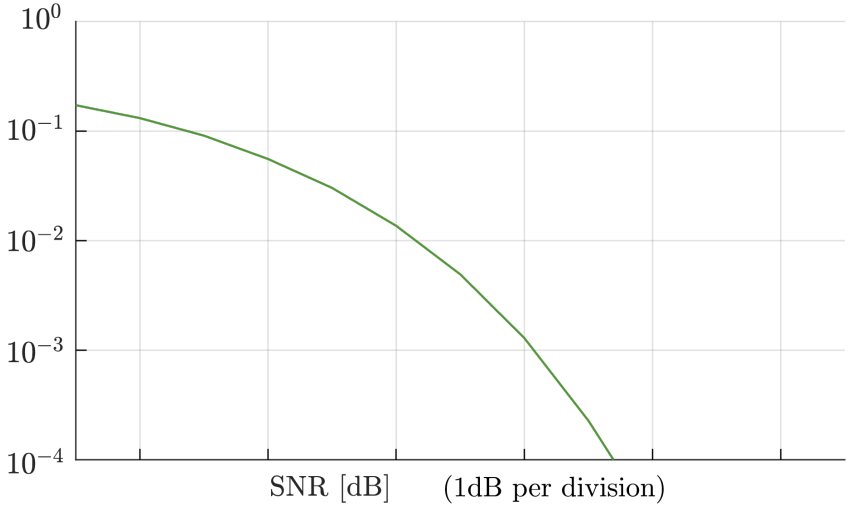

Figure B3: Matching aspect ratio to that of Fig. B1

INL FBMC-SS
Nordic FBMC-SS [2]
Walsh [2]

Appendix B: fitting in AWGN (cont.)

INL FBMC-SS
Nordic FBMC-SS [2]
Walsh [2]

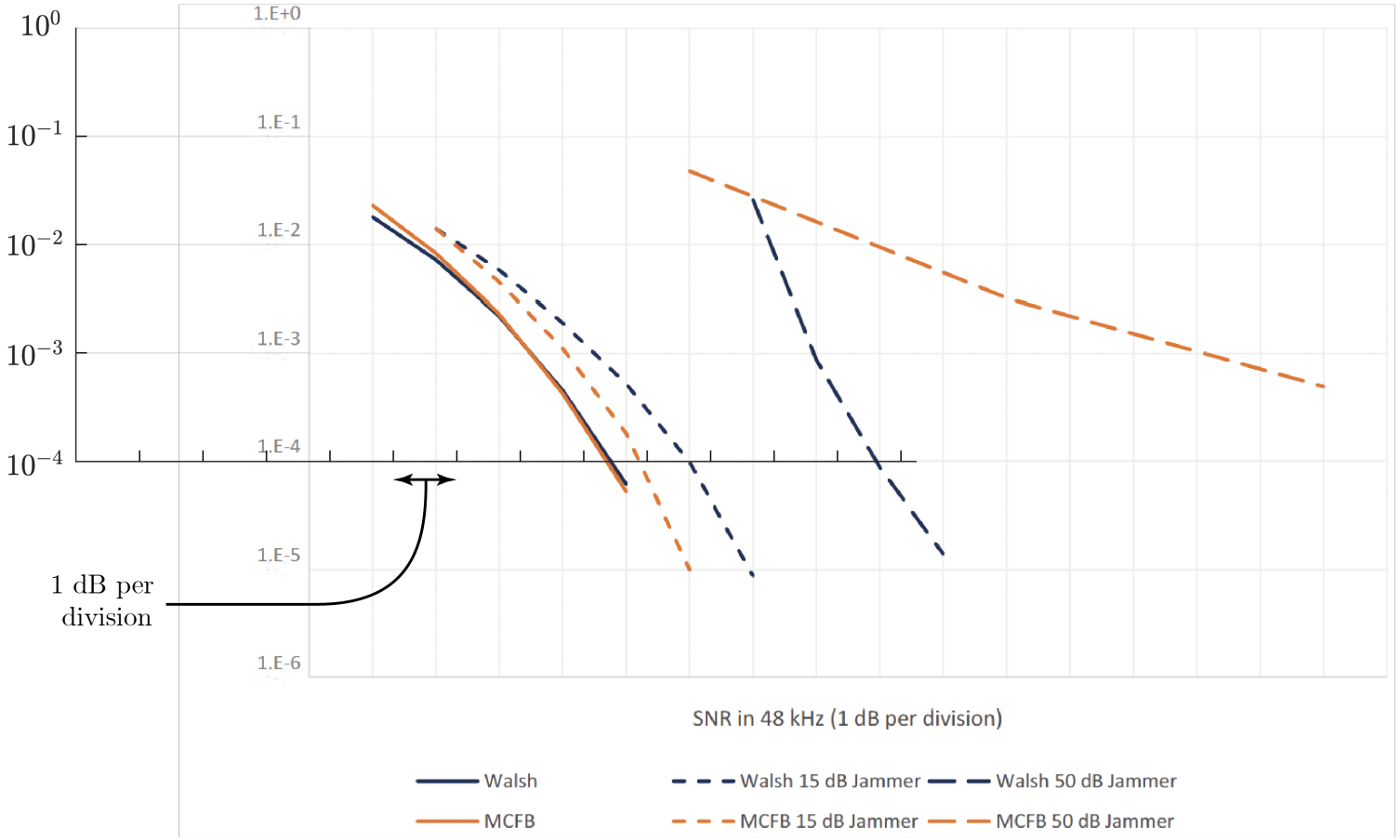

Figure B4: fit our axes to given Figure with performance of our implementation to provide approximate SNR values

Appendix B: fitting in AWGN (cont.)

INL FBMC-SS
Nordic FBMC-SS [2]
Walsh [2]

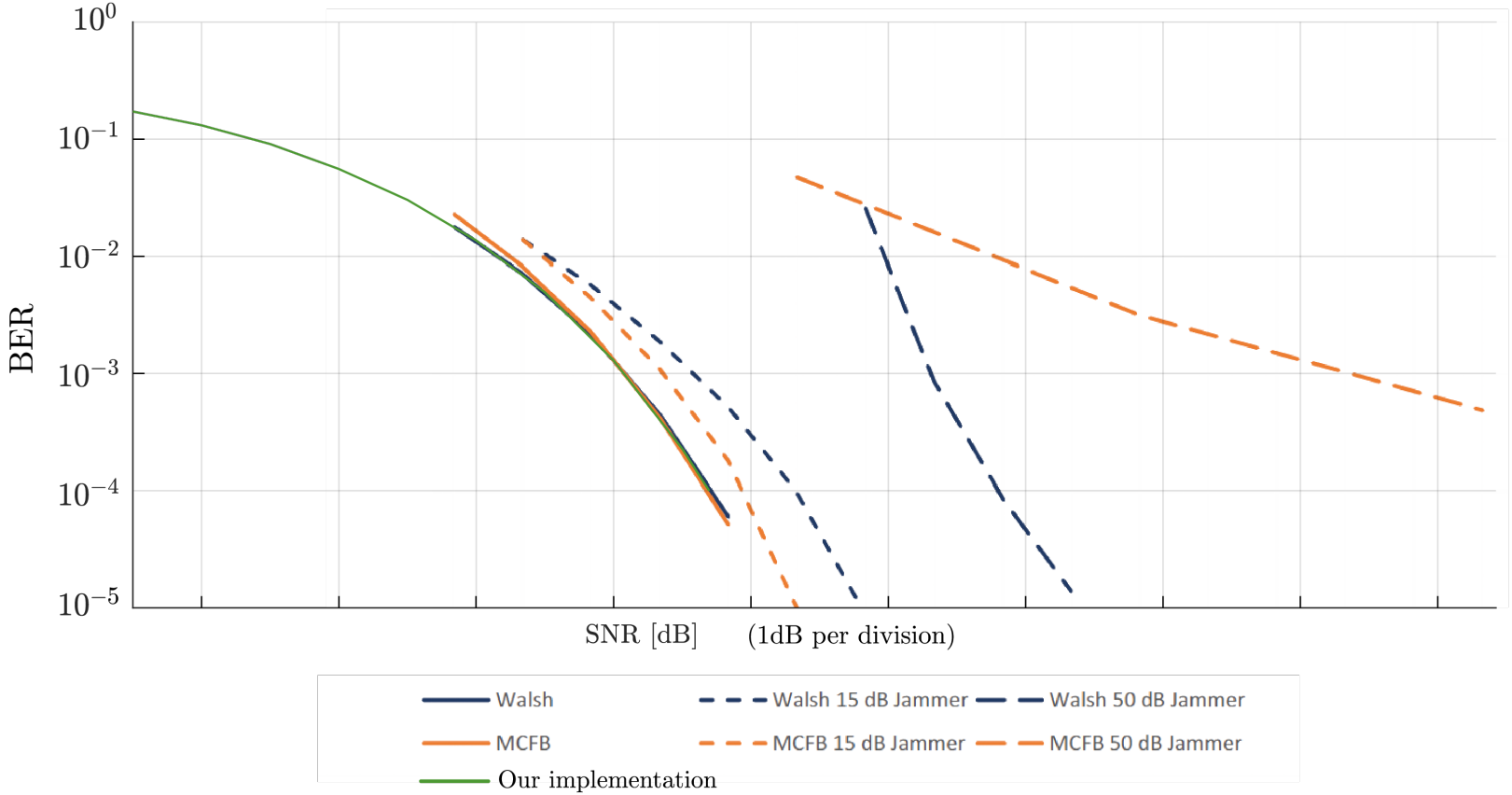

Figure B5: Unifying and extending axes

Appendix C: Severe, dynamic interference

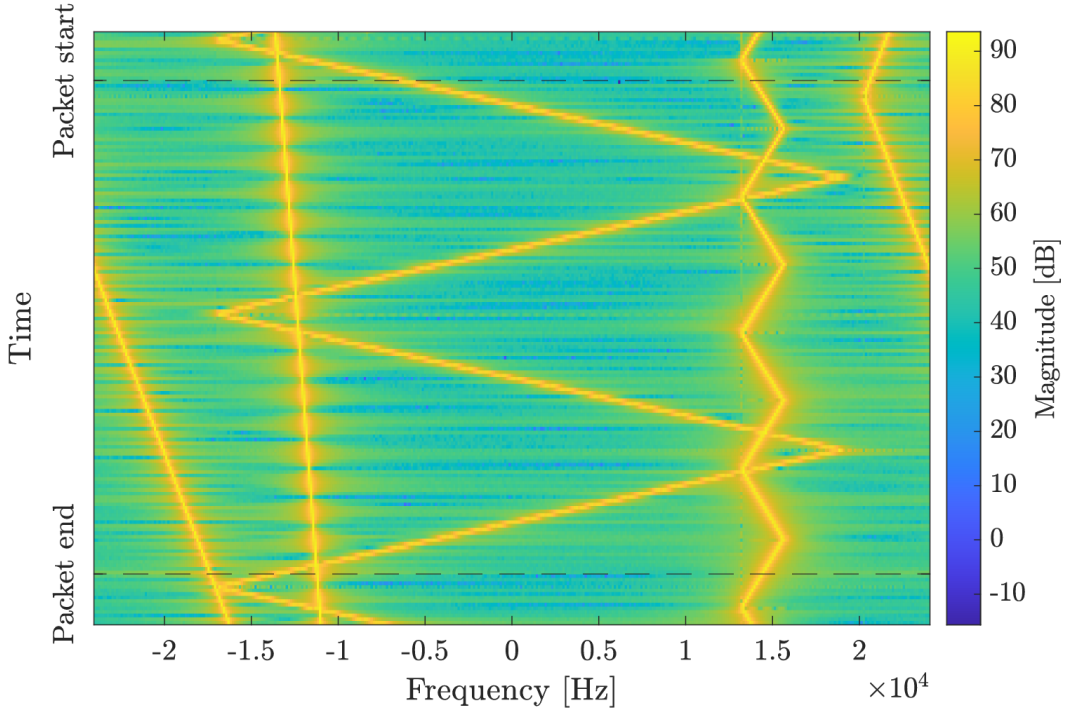

Figure C1: 4 swept tones polluting passband of FBMC-SS signal. Each tone has $P_{\text{intf}} = 50$ dB.

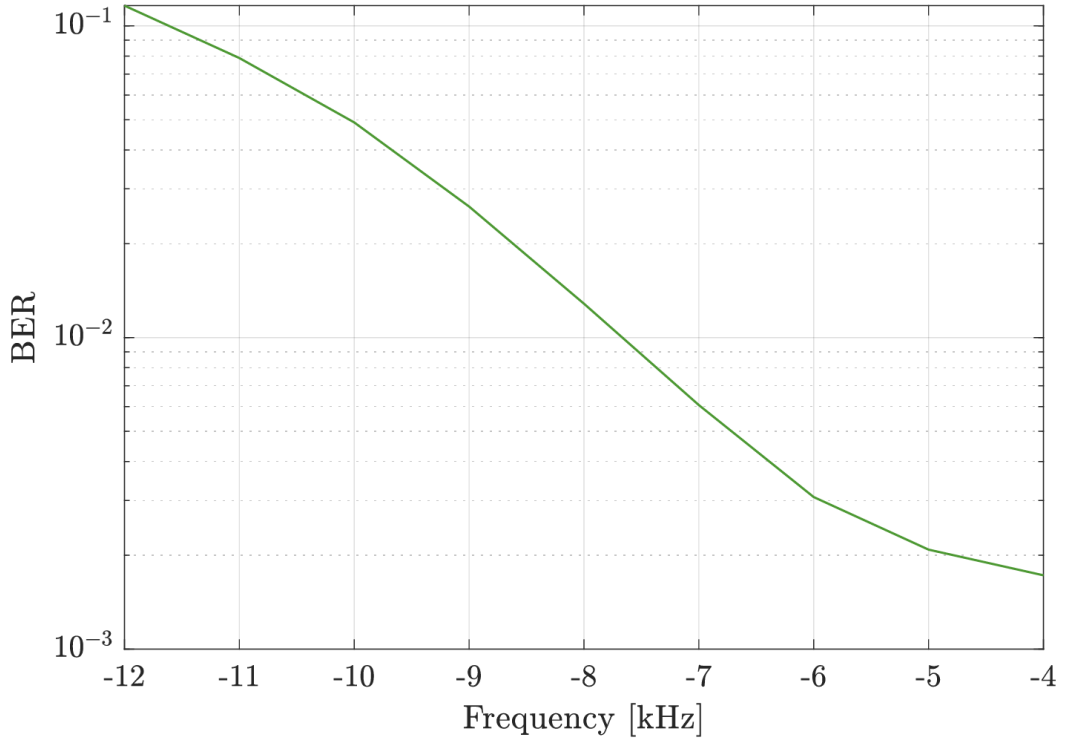

Figure C2: BER performance of FBMC-SS performance in interference scenario presented in Fig. C1.